UPCONVERSION NANOPARTICLES FOR PHOTODYNAMIC THERAPY

A Major Qualifying Project Submitted to the Faculty of

Worcester Polytechnic Institute

in partial fulfillment of the requirements for the

Degree in Bachelor of Science in

Biomedical Engineering

By

_____

Mahmoud El-Rifai

_____

Hyungseok Lee

_____

Amira Tokatli-Apollon

Date: 5/1/14

Sponsoring Organization:

University of Massachusetts Medical School:

Principal Investigator:

Dr. Gang Han

Project Advisors:

_____

Dr. Marsha Rolle, Advisor

Acronym Definitions

ALA:	5-aminolevulinic acid
A.U.:	Absorbance Unit
Ca:	Calcium
CaF_2:	Calcium Fluoride
CT:	Computer Tomography
CW:	Continuous Wave
DCFDA:	Dichlorofluorescein Diacetate
DI water:	Deionized water
DMF:	Di-methylformaide
EDC:	1-Ethyl-3-(3-dimethylaminopropyl)-carbodimide
Er:	Erbium
FDA:	U.S. Food and Drug Administration
FTIR:	Fourier Transform Infrared Spectroscopy
HBSS:	Hank's Balanced Salt Solution
HPLC:	High-performance liquid chromatography
Hyd:	Hydrazine
KBr:	Potassium Bromide
Ln:	Lanthanide
MTT:	Methylthiazol Tetrazolium
$NaYF_4$:	Sodium Yttrium Fluoride
$NaCF_3COO$:	Sodium Trifluoroacetate
Nd:	Neodymium
NIR:	Near Infra-Red
$NOBF_4$:	Nitrosonium tetrafluoroborate
OA:	Oleic Acid
OAm:	Oleyamine
ODE:	Octadecene-1
OH^-:	Hydroxide
PAA:	Polyacrylic acid
PBS:	Phosphate Buffer Saline
PDT:	Photodynamic Therapy
PET:	Positron Emission Tomography

PpIX:	Protoporphyrin IX
PS:	Photosensitizer
ROS:	Reactive Oxygen Species
TEM:	Transmission Electronic Microscopy
TFA:	Trifluoro-acetate
Tm:	Thulium
UC:	Upconversion
UCNP:	Upconversion Nanoparticle
UV:	Ultra Violet
Y:	Yttrium
Yb^{3+}:	Ytterbium
$1O_{2:}$	Singlet oxygen

Table of Contents

Acronym Definitions 2
Authorship: 6
Acknowledgements 6
Table of Figures 7
Chapter 1: Introduction 9
Chapter 2: Literature Review 11
Photodynamic Therapy (PDT) 11
Upconversion nanoparticles (UCNPs) 12
Combination of PDT & UCNPs 15
5-Aminolevulinic acid 16
ALA Advantages: 17
ALA disadvantages: 18
Chapter 3: Project Strategy 19
Initial Client statement 19
Objectives 19
Objective List 20
Design Constraints 22
Functions 22
Revised Client Statement 23
Project Approach 23
Upconversion Nanoparticle Size and its uniformity 24
Transducing near-Infrared into Visible light and Biocompatibility 25
Testing 25
Chapter 4: Alternative Designs 26
Requirements analysis 26
Objectives 26
Alternative designs 26
ALA Coupling 32
Chapter 5: Design Verification 36
Transmission Electron Microscopy (TEM): 36
Fourier Transform Infrared Spectroscopy (FTIR) Spectral Analysis 37
High-Performance Liquid Chromatography (HPLC) Analysis: 39

Methylthiazol Tetrazolium (MTT) Assay: 39
Cell Viability Exposed to 20% and 80% (MTT Assay) 40
Singlet Oxygen Detection Cell Imaging 41
Singlet Oxygen Detection Quantification 42
MTT Assay with Porcine Tissue 43
Chapter 6: Discussion 45
Viability and Effectiveness of UCNPs-ALA for PDT as cancer treatment 45
UCNPs for PDT as a cancer Treatment: A larger perspective 48
Economics 48
Societal Influence 48
Political Ramification 49
Health and Safety 49
Ethical Concern 49
Chapter 7: Final Design and Validation 51
Chapter 8: Conclusions and Recommendations: 54
Conclusions 54
Recommendations 55
References 57

Authorship:

Mahmoud, Hyungseok and Amira authored Chapters 1 and 2

Hyungseok authored Chapters 3, 4 and 8

Amira authored 5-Aminolevulinic acid section, Chapter 5, and Illustrations including Figure 1, 2, 3, 11, 12, and 22

Mahmoud authored Chapters 6 and 7

Mahmoud, Hyungseok and Amira contributed to the editing and formatting of the final report.

Acknowledgements

We would like to show appreciation to the following individuals for their unlimited assistance, advice, and guidance throughout the course of this Major Qualifying Project:

Dr. Gang Han of UMass Medical School, for his support in coordinating and sponsoring our research

Dr. Marsha Rolle of Worcester Polytechnic Institute, for her guidance, advice, and encouragement throughout the entirety of the project

Amol Punjabi, Xiang Wu and Yuanwei Zhang of UMass Medical School for their assistance and support for the completion of this project

Table of Figures

Figure 1. General Schematic of PDT mechanism 12
Figure 2. Upconversion Nanoparticle Diagram 13
Figure 3. Schematic of the ALA-UCNPs Entering the Cell 17
Figure 4. Objective Tree ..... **Error! Bookmark not defined.**
Figure 5. Pairwise Comparison Chart ..... **Error! Bookmark not defined.**
Figure 6. Project Cost Breakdown 24
Figure 7. 99.5%Yb 0.5%Tm Core nanoparticle with laser and TEM imaging 28
Figure 8. 99.5%Yb 0.5%Tm Core with $NaYF_4$ shell nanoparticle with laser and TEM imaging 29
Figure 9. Alternative designs; CaF_2 nanoparticles comparison with different ratio of Yb; 20%, 40%, 60%, 80%, and 98% respectively 31
Figure 10. TEM image of CaF2 nanoparticle with 80%Yb 2%Er 31
Figure 11. The Process of Conjugating 5-Aminolevulinic acid on αNaYF4:Yb80%Yb,2%Er@CaF2 34
Figure 12. Illustration demonstrating the Production of PpIX in the mitochondria . 35
Figure 13. Emission spectra (a) under CW 980 nm 1 W/cm2 excitation and photographs (b) of α-NaYF4:Yb,Er@CaF2 UCNPs with different Yb-levels (c) Integrated counts of red emission of α-NaYF4:Yb,Er@CaF2 UCNPs with different Yb-levels. 36
Figure 14. Characterization of hydrophilic UCNPs: TEM images of PAA-UCNPs (a), Hyd-UCNPs (b), ALA-UCNPs (c). Emission spectra of hydrophilic PAA-UCNPs in distilled water and hydrophobic OA-UCNPs in hexane, both at 10mg/mL (e) and integrated counts of their red emission indicating about 30% quenching. 37
Figure 15. Images of the FTIR Process 38
Figure 16. Full FTIR spectra (A) and partial detailed spectra (B) of PAA-, Hyd-, and ALA-UCNPs. 39
Figure 17. HeLa cell viability exposed to ALA-UCNPs (100 μg/mL), Hyd-UCNPs (100 μg/mL), free ALA (100 μg/mL), and nothing (growth control) and irradiated with CW 980 nm light at 1W/cm2 power density 40

Figure 18. HeLa cell viability exposed to 20% Yb and 80% Yb ALA-UCNPs (100 μg/mL) and 20% Yb and 80% Yb Hyd-UCNPs (100 μg/mL) and irradiated with CW 980 nm light at 1W/cm2 power density. 41
Figure 19. Singlet oxygen production detected by fluorescence of DCFDA in HeLa cells exposed to 100 μg/mL of ALA-UCNPs and irradiated with 0 (a), 5 (b), and 10 (c) minutes of CW 980 nm light at 1W/cm2 power density. Singlet oxygen production detected by fluorescence of DCFDA in HeLa cells exposed to 100 μg/mL of Hyd-UCNPs and irradiated with 0 (d), 5 (e), and 10 (f) minutes of CW 980 nm light at a 1W/cm2 power density. 42
Figure 20. Singlet oxygen quantified by DCFDA fluorescence in HeLa cells exposed to 100μg/mL of ALA UCNPs, Hyd-UCNPs, ALA, and nothing (growth control). 43
Figure 21. Photograph of the setup of simulated visceral tumor conditions in an in vitro MTT assay (a). HeLa cell viability exposed to ALA-UCNPs (100 μg/mL) and Hyd-UCNPs (100μg/mL) and irradiated with CW 980nm light at a 1W/cm^2 power density for 20 minutes 44
Figure 22. Schematic of the final design components and its work mechanisms 51

Chapter 1: Introduction

Cancer is an uncontrolled growth of cells in the human body. It is the second leading cause of death in the US, with 1,660,290 new expected cases and about 580,350 expected to die in 2013 (*American Cancer Society, 2012a*) . Cancer has a variety of treatments, and the most effective ones are chemotherapy, radiotherapy and surgery, but all of these treatments are not ideal in every cancer case, especially in the later stages when metastasis occurs. Due to the side effects that cancer treatments have, scientists are always looking to improve current treatments and find better alternatives. (*American Cancer Society, 2012b*)

Photodynamic Therapy (PDT) with Upconversion Nanoparticles (UCNPs) is a treatment that shows significant potential in this field. PDT is a treatment that uses a photosensitizing agent. When photosensitizers are exposed to a visible wavelength of light, they produce singlet oxygen ($1O_2$) that kills nearby cells; it has been used mostly for skin diseases (*Dougherty, 1998*).

UCNPs, is a mixture of lanthanide-doped nano-crystals, which emit high energy photons and visible light under excitation by near-infrared (NIR) light. Therefore UCNPs will act as transducers, absorbing NIR light and converting it to visible light, which is essential in PDT to activate the photosensitizer drug and release singlet oxygen to kill cancer cells. Using both PDT and UCNPs for cancer treatment showed promising results, especially in In-vivo testing (*Wang, 2010*).

The UCNPs that have been used with PDT for cancer treatment were excited at 980nm wavelength, which showed good results (*Idris, 2012*). Ytterbium (Yb^{3+}) sensitizer is the element commonly used for its unalterable excitation band centered at 980nm. However, a longer wavelength from the UCNP with NIR causes the exciting light to penetrate deeper into the biological tissue.

5-aminolevulinic acid (ALA) is currently used clinically in PDT as an FDA approved photosensitizer drug. Through heme biosynthesis, ALA has a hydrophilic characteristic and selectivity for photosensitizer protoporphyrin IX (PpIX) production in cancer cells, and triggers and generates the red-absorbing photosensitizer PpIX. ALA was found to be a suitable agent with the UCNPs designed by the team. It is important to note; however, ALA usage in PDT requires the emission of red light, which here is converted from NIR light by the UCNPs, in order to activate PpIX.

Therefore, the aim of this project was to enhance the use of photodynamic therapy with nanoparticles by designing UCNPs with different percentages of Yb^{3+} in their cores, which modifies the level of excitation and red emission at 980nm wavelength. The team had reproduced 99.5% Yb and 0.5% Tm UCNPs with blue light emission to learn the techniques and skills that are needed to create UCNPs, then started producing Calcium Fluoride (CaF_2) shell with different ratios of Yb% in UCNPs core due to its biocompatibility and promoting more red visible light, looking for possible alternative designs by comparing the chemical effects of various percentages of Yb^{3+} used when creating the UCNPs.

With the five alternative designs, which used 20%, 40%, 60%, 80%, and 98% Yb^{3+} contained in CaF_2 UCNPs, the team performed a variety of experiments to verify which designs would satisfy requirements. Transmission Electron Microscopic (TEM) images were obtained in order to check the CaF_2 particle sizes and uniformity, then emission spectra data were acquired to check its quantitative values of its emission brightness. Also, Fourier Transform Infrared Spectroscopy (FTIR) and High-performance liquid chromatography (HPLC) were performed to check the completion of ALA-synthesis. In addition, cell viability; Methylthiazol Tetrazolium (MTT) Assay was also performed to verify toxicity within HeLa cells. Along with toxicity testing, Cellular Reactive Oxygen Species Detection Assay using Dichlorofluorescein Diacetate (DCFDA) was performed to measure the singlet oxygen production. As the final stage of verification, the team performed MTT assay with porcine tissue to check emission penetration.

Chapter 2: Literature Review

The aim of this chapter is to explain and describe the basic concepts of Photodynamic therapy (PDT), Upconversion Nanoparticles (UCNPs), and the combination use of PDT with UCNPs the benefits and drawbacks.

Photodynamic Therapy (PDT)

Photodynamic therapy is a non-invasive treatment where involves three main components. These components are; the laser with different wavelength, the photosensitizer (PS) molecules, and the production of singlet oxygen (*Wang, 2013*). Desired laser with a different wavelength used directly on targeted cells as a source of light, this will activate the PS drug causing the production of singlet oxygen, leading to the generation of reactive oxygen species (ROS), which is toxic product causing damage to cellular components (*Sharman, 1999*).

PDT was used in many clinical trials, the first successful application was recorded for curing acne by using ultra-violet (UV) light (*Kalka, 2000*). For many scientists and researchers the achievement using PDT drew attention to the important use in different medical fields such as cancer treatment since it was the biggest challenge this day. Cancer studies using PDT showed positive results of substituting major cancer therapeutic treatment from chemotherapy and radiotherapy with the PDT (*Moan, 2003*).

When the PS absorbs the UV light, the PS goes into a high energy state, transferring this energy to the surrounding molecules causing the production of singlet oxygen ($1O_2$) or other reactive oxygen species. The ROS species are very toxic and has the ability to destroy tumors by either direct cancer cell death by necrosis, apoptosis (*Oleinick, 2002*), or by damaging tumor vasculatures as an anti-angiogenesis effect (*Fingar, 1996*).

The common procedures of PDT treatment starts with injecting drug with the PS in a proper delivery system. Once the delivery system spread over a patient's body, it causes drugs to remain at the tumor tissue long period of time than healthy tissues. Then a certain laser will be shed upon the area of tumor, which activates PS to release harmful chemicals to kill tumor cells as shown in the Figure 1 below. Throughout the excretory system of the patient's body, the gradually clearance of the drug in the body, and the decrease of the volume of the tumor will be done (*Kalka, 2000*).

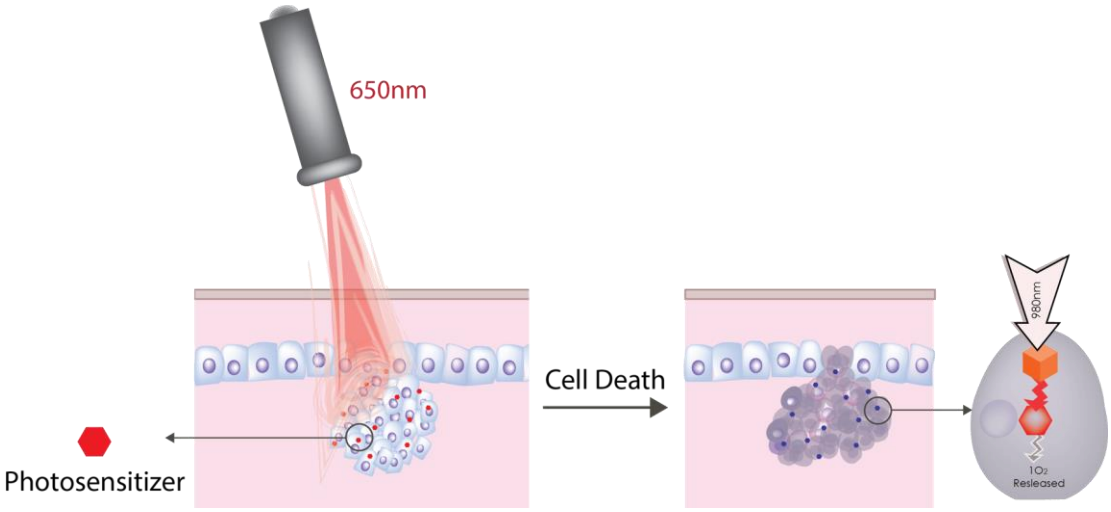

Figure 1. General Schematic of PDT mechanism

Even though PDT had successful results, it had a poor tissue penetration due to the lack of light transmission and severe photo-toxicity (*Sharman, 1999*). Most PDT PS molecules currently used are excited by visible or UV light, which has limited penetration depth in biological tissues, therefor this poor tissue penetration will limit the use of PDT in treating large or internal tumors (*Yang, 2012*).

Upconversion nanoparticles (UCNPs)

Upconversion Nanoparticles (UCNP) are usually composed with core and shell as shown in figure 2 below. Core part of the UCNP, which mostly have a sphere shape, allows the process in which the sequential absorption of two or more photons leads to the emission of light at shorter wavelength than the excitation wavelength. By properties of the composition of core structure, it would have different wavelength of near infra-red (NIR) light convertibility and the color of visible light produced. UCNP shell functions to affecting to have various intensity of emission and suitable material's purposes from the Core by having the photosensitizers loaded on host matrix of itself. The mechanisms of UCNP are accomplished in solid-state materials doped with rare-earth ions, where it convert long-wavelength radiation like infrared or near NIR, to a short-wavelength radiation (*Haase, 2011*).

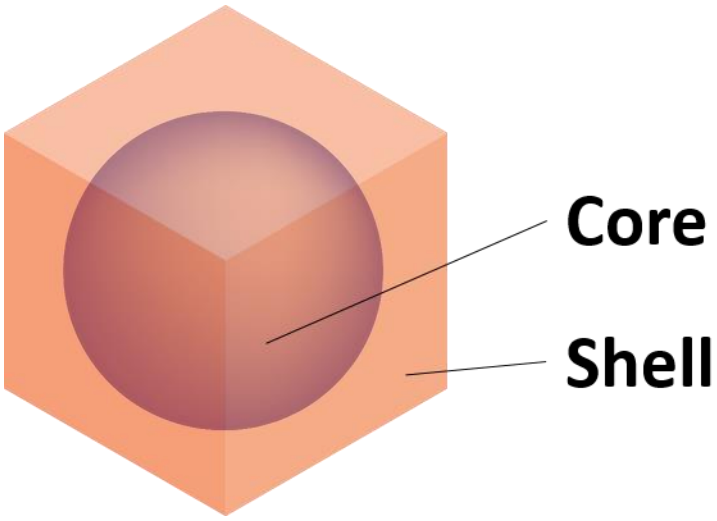

Figure 2. Upconversion Nanoparticle Diagram

Using lanthanide-doped solids showed high Upconversion efficiencies at a room temperature. Upconversion nanoparticles are usually made of host lattices of ceramic materials, such as LaF_3, YF_3, Y_2O_3, $LaPO_4$, $NaYF_4$ embedded with trivalent lanthanide ions like Yb^{3+}, Er^{3+}, and Tm^{3+} and show a unique phenomenon of absorbing NIR light and emitting UV, visible, and NIR light (*Xueyuan,2014*). The most effective lanthanide (Ln)-doped UCNP containing host Sodium Yttrium Fluoride ($NaYF_4$) matrix, sensitizer Ytterbium (Yb^{3+}) and emitter Thulium (Tm^{3+}) ions (Haase, 2011), where it can absorb NIR light from a continuous wave (CW) and emit photons at shorter wavelengths that extend to the UV region (*Shen, 2013*). When UCNPs excited by the Near-Infrared light it will absorb the light and transfer it to the core emitting visible and UV light.

In addition, UCNPs show a sharp emission bandwidth, long half-life time, tunable emission, high photo-stability, low cytotoxicity, Nano-scale size, visible emission under NIR light excitation, greater tissue penetration and the ability for protein attachment as well as surface modification used in different biological and clinical applications (*Chen, 2012*). Recently, these properties of the UCNPs increases its variety in different usages as its purposes (*Wang, 2011*).

UCNPs has the potential to be used in many different applications like cell imaging, photodynamic therapy, drug delivery and many other applications, since each task is different than the other changing the surface molecules for UCNPs is essential procedure to make hydrophilic UCNP with pendant functional groups, which will give the ability of UCNPs to be used in living organisms. Due to UCNPs' various types of possible ligand

exchanges on the shell surface, ligand engineering involves a ligand exchange reaction with hydrophilic bi-functional molecules or involves a direct oxidation of the terminal group of native ligands to generate a pendant carboxylic functional group. Ligand attraction involves absorption of an additional amphiphilic polymer onto the nanoparticle surface through the hydrophobic Van der Waals attraction between the original ligand and hydrocarbon chain of the polymer. Surface polymerization involves growing a dense cross-linked shell on the nanoparticle core by condensation of small monomers. Last but not least Layer-by-layer assembly involves electrostatic absorption of alternately charged poly-ions on the nanoparticles surface. These entire synthetic procedures yield to hydrophilic UCNPs, which could have additional functional groups and further bio-conjugation capabilities (*Wang, 2013*).

As the first use of UCNP's NIR-to-UV convertibility, Zhang and his team reported NIR-to-UV β-$NaYF_4$, 25%Yb^{3+}, 0.3%Tm^{3+} UCNPs for photo-controllable gene expression (*Jayakumar, 2012*). Photo-caging is any one of several molecular species that can be activated by light; they are used especially in biochemistry to attach a molecule to a biologically active compound and then study its behavior once activated. Photo-caging involves the caging of molecules of interest by a light-sensitive molecule which can then be destroyed by light irradiation to make it functional. Various molecules, like proteins, peptides, nucleic acids, amino acids, and drugs, have been photo-caged and delivered to animal's cells and photolysis is done in the area of interest, enabling activation of these molecules with very high spatial and temporal resolution. Due to the limitation of photo-activating systems it can be only use in in-vitro applications, because UV light necessary for the uncaging process, which is very harmful, besides having a poor tissue penetration depth, which made it useless for in vivo and clinical use.

NIR light has the deepest tissue penetration compared to visible and UV light. It is also safe and is expected to cause minimal photo-damage to the biological specimen involved Zhang and his team chose to use UCNPs to convert NIR to UV light. Due to the thin layers of mesoporous silica and caged DNA/siRNA in the mesopores, delivery of higher payload and protection of the nucleic acids from the harsh environment was possible. The method that Zhang and his team used has many advantages to improve photo-caging by increasing the loading efficiency of nucleic acids when compared to chemical

crosslinking. The degree of activation reduces with increase in thickness of the tissue but significant activation more than 50% was seen even with a tissue phantom thickness of 0.4 cm. Data provided by the team showed more efficient loading and delivery of the DNA/siRNA cargo molecules.

The results support the team hypothesis, which showed the necessity of using UCNPs for photo-controllable gene expression is that NIR to UV by using UCNPs, which can be used for activating photo-caged nucleic acids in deeper tissues compared to conventional systems. The results prove that this technique has enormous potential in a variety of fields such as gene therapy and specific gene delivery or knockdown.

Combination of PDT & UCNPs

PDT based on UCNPs has a major advantage of targeting and treating such a deadly disease as cancer. UCNP is the process of converting two or more low energy photons to higher output photons. UCNPs have several properties useful in PDT due to its emission ability upon a low level of excitation in the NIR of the spectral region including sharp emission bandwidth, long lifetime, tunable, high photo-stability as well as lower cytotoxicity. Upon UCNP excitation using NIR light converting longer wavelength into emission at a shorter wavelength in UV, visible or, NIR light, which can activate loaded photosensitizers molecules to produce singlet oxygen killing cancer cells that is more specific to a nanometer regime with minimal photo damage and a significant enhancement in light penetration depth.

Coated $NaYF_4$ UCNP with mesoporous silica were irradiated using a 980nm laser causing the loaded drug to release singlet oxygen ($1O_2$). The $1O_2$ is known for its toxicity to targeted cells such as cancer cells. After evaluating the efficiency of the UCNP as a PDT agents in in vitro by minimizing the volume of cancer cells caused by the toxicity of $1O_2$, Idris and his lab proceeded an In-vivo experiments (*Idris, 2012*). Melanoma cell coated UCNP injection subcutaneously to mice in four different conditions; UCNP loaded with drug then irradiated with a 980nm laser, UCNP loaded with drug, no drug with a laser exposure of 980nm, and untreated. After two weeks, cells except UCNP loaded with drug then irradiated with a 980nm laser condition formed a solid tumor while cells in group 1 has considerably been decreased. Current UCNP based PDT application achieved data

success, but this process is still limited due to insufficient upconverting efficiency of the nanoparticles.

5-Aminolevulinic acid

As discussed in Chapter one, PDT is based on three important elements; light, $1O_2$ and a photosensitizer. Photosensitizer is a very important for photosensitization efficacy and producing $1O_2$. Once light gets absorbed, it causes excitation of molecules, which activates the photosensitizer (*Tian, 2013*). PDT can be a new approach of using an endogenous photosensitizer protoporphyrin IX (PpIX). PpIX is known as the precursor of prophyrins, which are naturally occurring organic compound. One of the most known prophyrins is heme; the co-factor of the protein hemoglobin. PpIX is an excellent photosensitizer due to its minimum to no photodynamic damage.

5-aminolevulinic acid (ALA) is one of the two FDA approved photosensitizers and clinically used. When ALA is administrated, it acts as a prodrug. ALA synthesis occurs in the mitochondria formed by the condensation of glycine and succinyl CoA, catalyzed by ALA-synthase. ALA undergoes several synthetic steps after it is transported into the cytosol. The transportation of cytosol causes the production of proto-prophyrins, then precursor prophyrinogens, protoporphyrin IX and then heme. As the final stages of heme biosynthesis, co-proporphyrinogen gets transported from the cytosol into the mitochondria and there converted to prophyrin and PpIX with an iron inserted (*Huang, 2005*).

ALA is an appropriate solution for cancer therapy because of its specificity for cancer cells. When ALA administrated exogenously, it acts as a prodrug generating photosensitizer PpIX via heme biosynthesis pathway in the cancer cells. The ALA-PDT depends on the generation of PpIX, which is the intermediate of heme biosynthesis and does not accumulate in the pathway. Generating more PpIX quantities required; therefore, ALA administrated exogenously with an active heme biosynthesis, the pathway becomes temporarily overloaded. The control mechanism is bypassed, and downstream metabolites are synthesized in excess. Next, the ferrochlelatase; catalyze in the biosynthesis of heme where it is convert pro proporphyrin IX into heme with insertion of iron. PpIX accumulate in the cells because of the low physiologic rate of iron insertion by ferrochelatase, which is unable to compensate for the excess PpIX formed and render them photosensitive (*Peng, 1997*).

Following, the synthesis of 5-ALA induced in mitochondria, the PpIX selectively accumulate in mitochondria causing the death of cells after PDT treatment. ALA has excellent intestinal absorption when administrated orally. ALA uses the intestinal and renal apical peptide transporters to enter epithelial cells and in some cells ALA is transported using system Beta transporters.

There are various theories explaining why ALA has a tendency to accumulate in tumors and other lesions. ALA tumor accumulation could be caused due to the low level of ferrochelatase in comparison with normal cells where less PpIX covered to heme, plus tumors have a low pH causing more PpIX retention leading to PpIX accumulation (*Collaud, 2004*).

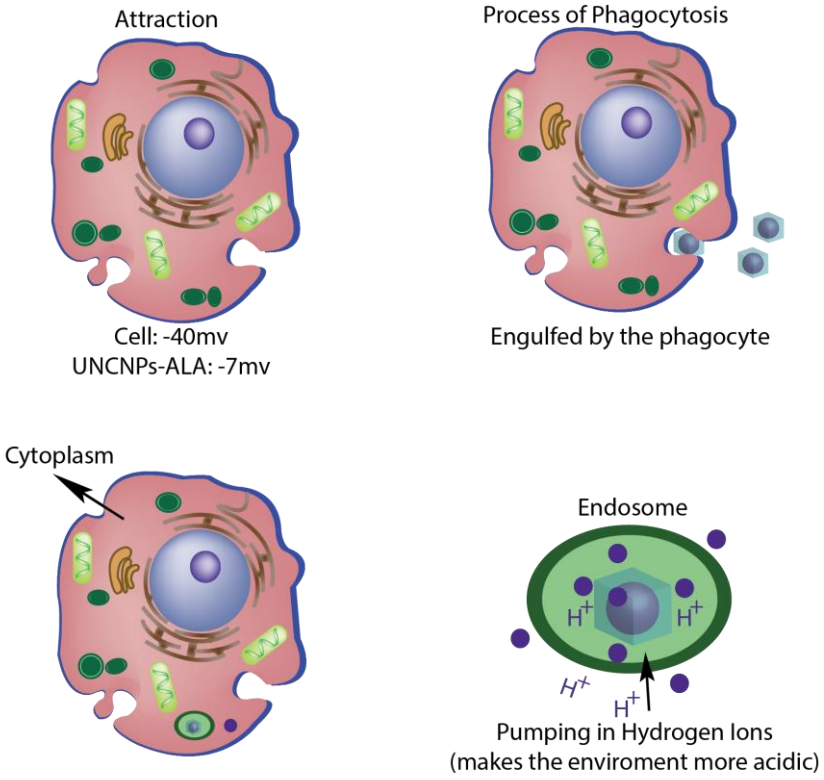

Figure 3. Schematic of the ALA-UCNPs Entering the Cell

ALA Advantages:

- Ability to penetrate the abnormal tumor under Stratum Corneum due to its small size and solubility
- ALA-PpIX accumulate in cells and not the tumor vasculature
- Rapidly cleared from the system 1-2 days

- Easily synthesized
- ALA- PDT is noninvasive treatment, where it does not harm surrounding tissue
- ALA can be administrated topically

ALA disadvantages:

- ALA has low lipid solubility, therefore has a limited ability crossing biological barriers
- PpIX limited tissue penetration 1mm
- ALA stable is an acid environment, pH low as 2-2.5.

Chapter 3: Project Strategy

In this chapter, each planned procedures prioritized by the various objectives and constraints will be introduced. The project approach section will also explain the project framework of necessary steps to complete the proposed Upconversion Nanoparticle (UCNP) Synthesis.

Initial Client statement

The following initial client statement was given from the client, Dr. Gang Han from University of Massachusetts Medical School.

> "Photosensitizers are excited by visible or Ultra Violet (UV) light, which has limited penetration depth due to the light absorption and scattering by biological tissues, resulting in ineffective therapeutic effects to internal or large tumors. UCNPs have the ability to convert Near Infra-Red (NIR) light to visible photons, which can active photosensitizers adsorbed on nanoparticles via resonance energy transfer to generate singlet oxygen ($1O_2$) to kill cancer cells. It would provide an alternative to overcome hurdles of current photodynamic therapies. The goal of this project is to improve current UCNPs at a single excitation wavelength between 600nm and 1,200nm created by continuous-wave (CW) laser in order to perform better at imaging and safer to use with photodynamic therapy in living organisms."

Therefore, more research about photodynamic therapy (PDT) and UCNP has been performed. Then, the team arranged meetings and client interviews to better understand and clarify the initial client statement. Sets of objectives and constraints were listed to draft a revised client statement, which stated the client's problem and their desired solutions more concisely and clearly.

Objectives

Through research, the team discovered much information regarding upconversion nanoparticles (UCNPs) and Photodynamic Therapy (PDT). With the information, various objectives were brought up based on a compiled a list of current problems with UCNPs.

After analyzing the client statement, researching UCNP, and scheduling client meetings, the following list of objectives were made.

Objective List

- Particle size
- Particle uniformity
- Capable of upconverting NIR light to red visible light
- Deliver 5-aminolevulinic acid (ALA) to cancer cells

Based on the aforementioned list, an objectives tree was organized. In the objective tree, objectives of higher priority such as particle sizes, particle uniformity, capable of upconverting NIR light to red visible light, and deliver 5-aminolevulinic acid (ALA) to cancer cells were essential requirements of the client's need. Both particle size and uniformity were chosen for their direct relationship with biocompatibility. Either out of the given size range or non-uniform shape and size would lose their efficacy and increase cytotoxicity in human usage. Also, brighter red visible light transduction will be useful since PDT in deeper tissue would have low NIR light power due to the skin penetration. Finally, ALA is one of the most important component in PDT due to its role of activating photosensitizers to actually kill the cancer cells. Targeted cancer cells, in living organisms, bound with UCNPs and later excited with lasers eliminate the issue of $1O_2$ production. As a result, the objectives lay out the critical foundation for the most effective solution.

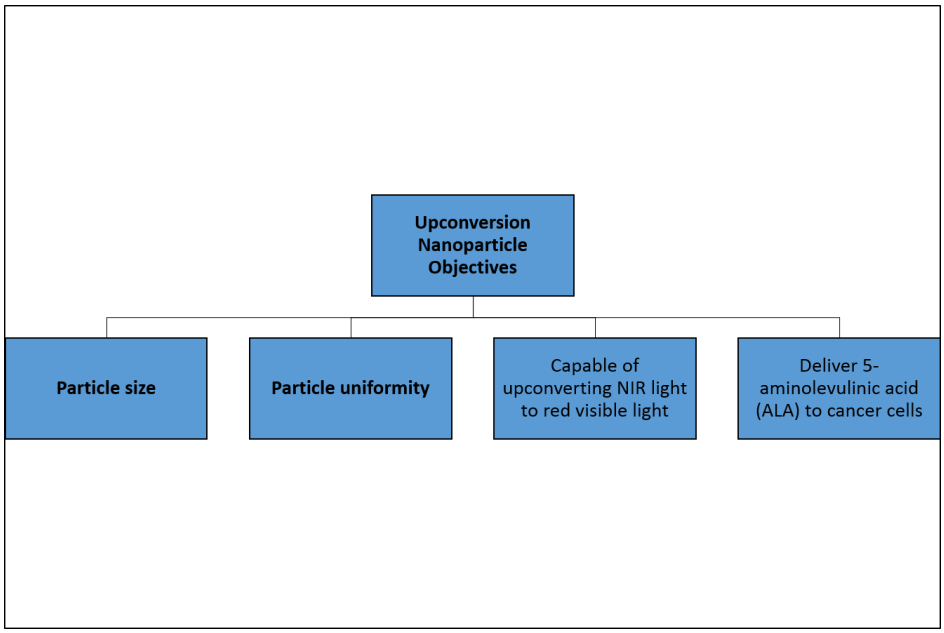

Figure 4. Objective Tree

All listed objectives were organized into a pair-wise comparison chart to rank team's objectives in order. The objectives of highest priority were compared with other objectives of highest priority. Each score of 1, 0.5, and 0 was assigned to objectives of high, medium, and low priorities.

	Particle size	Particle uniformity	Capable of upconverting NIR light to red visible light	Deliver 5-aminolevulinic acid (ALA) to cancer cells	Total
Particle size		0	0	1	1
Particle uniformity	1		0	0	1
Capable of upconverting NIR light to red visible light	1	1		1	3
Deliver 5-aminolevulinic acid (ALA) to cancer cells	0	1	1		2

Figure 5. Pairwise Comparison Chart

As shown in the pairwise comparison chart in figure 5 above, brighter red visible light was the most important objective, followed by suitable drug carrier of ALA. While

both particle size and uniformity were deemed important, they were considered secondary objectives.

Design Constraints

Constraints served to determine the real-world effectiveness of designed ideas. Failure to meet constraint criteria resulted in an automatic failure of a proposed solution. In light of the prior analysis of project requirements and lab research of the boundaries of UCNPs as a solution vector, the following list of constraints were made.

- Must have particle size within a range of 20-40nm
- Must have uniform particle diameter sizes with lower the standard deviation value less than 5nm
- Must transduce the wavelength between 700 to 1,100nm NIR light into visible red light more than 1.00×10^{8} absorbance unit (A.U.)
- Must be proven to be non-toxic through Methylthiazol Tetrazolium (MTT) assay
- Must reduce cell viability with 12mm thickness of tissue penetration through MTT assay
- Must have stable ALA-conjugation

In order to have UCNPs fulfill solution scope requirements, the diameter size of the particles must consistently be within a range of 20-40nm while responding to lasers emitted at a wavelength of 700 to 1,100nm. The design must also demonstrate non-toxicity within the body until exposure to controlled activation conditions.

Functions

Based on the constraints the team came up with, there were some specific functions, which the modified upconversion nanoparticle (UCNP) has to have. After analyzing the client statement, researching UCNP, and having a client meeting, the following list of functions can be listed.

In light of the aforementioned objectives and constraints, a formal list of functions that the team's modified UCNPs must have was drafted.

- Produce strong red visible light brighter than 1.00×10^8 A.U.
- Perform non-toxic activity through cell viability assay
- Release $1O_2$ only when it shed with a certain NIR laser

In order to utilize UCNPs for the treatment of cancer under the tissue, it needed to transduce NIR laser into strong red visible light in order to activate the photosensitizer the controls the release of toxins to kill cancer cells.

Revised Client Statement

Based on the results of all the mentioned objectives, constraints, and functions above, a revised client statement was written. This statement helped the team successfully propose a promising design as well as identify potential design alternatives.

> "The goal of this project is to build upon current UCNP procedures so that it will result in a stable and effective method of treatment for subcutaneous cancer through increased light penetration and emission for ALA activation with designed wavelength excitation between 600nm and 1,200nm."

Project Approach

With the foundation of the project clearly defined, a project approach was then drafted to guide the Upconversion Nanoparticle synthesis project. After establishing objectives, constraints, and project goal, the next step was careful design. Due to the complexity of synthesizing UCNPs, the team familiarized themselves with the production procedures. Background research was conducted to fully understand the various chemical compounds and their characteristics in chemical reactions. Due to financial limitations in acquiring the necessary chemicals, as shown in figure 6 below, each compound candidate was carefully and thoughtfully handled in order to minimize chemical utilization while maximizing sample result usefulness. Lab equipment and space was provided by University of Massachusetts Medical School.

Upconversion Nanoparticle Production Cost (50 X 5 ml of production cycles)

Chemical Compound Category	Amount Required	Unit*	Unit Price*	Total
Sodium Trifluoroacetate Na(CF3COO)	100g	100g	$79.10	$79.10
Ytterbium Trifluoroacetates Yb(CF3-COO)3	50g	10g	$131.40	$657.00
Thulium(III) trifluoroacetates $Tm(CF_3COO)3$	50g	25g	$630.00	$1,260.00
Neodymium (Nd)	50g	10g	$148.40	$742.00
Oleic Acid (OA)	1,000 ml	1,000 ml	$70.00	$70.00
Oleylamine (OAM)	1,000 ml	500 ml	$97.60	$195.20
1-Octadecene (ODE)	2,000 ml	1,000 ml	$28.90	$57.80
			Total Chemical Compound Cost	**$3060.90**

Disposable Lab Equipment Category	Amount Required	Package*	Package Price*	Total
50mL Conical Centrifuge Tubes	150 Pcs	500 Pcs	$326.00	$326.00
			Total Disposable Lab Equipment Cost	**$326.00**

Price for 5ml of UCNPs = $67.7

Total Production cost	**$3,386.90**

Figure 6. Project Cost Breakdown

Upconversion Nanoparticle Size and its uniformity

Biocompatibility and biodegradation were the highest priorities for the project. To achieve this goal, it was imperative that the diameter of the created UCNPs stay between 20nm to 40nm. ALA conjugation on UCNPs added another 10nm increase in diameter which would place the UCNP at the ideal range of 30nm to 50nm. A diameter less than 30nm would result in reduced effectiveness as a drug carrier within the human body while a diameter higher than 50nm would result in an inability to penetrate tissue and loss of biocompatibility. UCNPs designed to have diameters of 26nm (with a standard deviation of 2nm) were designed for use in experiments. However, due to the sensitivity of UCNPs, differing materials and procedures effected the size and consistency of the UCNP solutions. Furthermore, the molar ratio of components and the amount of Sodium Trifluoroacetate (NaCF3COO) affected the size of the particles with more NaCF3COO resulting in increased diameters and less NaCF3COO resulting in decreased diameters. To maintain uniformity within the UCNP solutions, exacting temperature application had to be enforced. Transmission Electronic Microscopy (TEM) was then used to gather results, which were then statistically analyzed.

Transducing near-Infrared into Visible light and Biocompatibility

Cancer cells are commonly located under the skin at a depth of roughly 12mm or even deeper. In order to utilize UCNPs as treatment, a NIR laser of a 980nm wavelength proved the best candidate. After successfully penetrating the skin with the NIR laser, the UCNP compound must convert the energy into bright red visible light to trigger the activation photosensitizer that controls the release of $1O_2$. The light emitted from the UCNPs, upon activation, must be brighter than $1.00x10^8$A.U. Also, compound selection requires biocompatibility, which promotes opsonization of reticuloendothelial system.

Testing

Utilizing TEM imaging and Emission Spectra analysis, the team rooted out a promising final candidate amongst all the proposed designs. In-vitro tests were then performed followed by another round of TEM imaging to check for correct ALA conjugation of UCNPs to determine the final size and uniformity. Once those two tests were completed, a round of Fourier Transform Infrared Spectroscopy (FTIR) was performed to verify the stability and conjugation status of the UCNPs. Next, to determine whether or not the UNCPs were correctly releasing $1O_2$, Fluorescence Intensity of Cellular Reactive Oxygen Species Detection Assay (DCFDA) was performed. After the confirmation of the release of singlet oxygen, the final design with ALA conjugation was then injected directly into a cell culture medium for Methylthiazol Tetrazolium (MTT) Assay using HeLa cells. 12mm of porcine skin, which was obtained from a grocery market, was then used to simulate human skin tissue and determine the effectiveness of the ability of the 980nm wavelength laser to penetrate skin tissue. Despite passing through 12mm of skin, the 980nm laser was still able to activate the photosensitizers. These experiments were then repeated three times for statistical analysis.

Chapter 4: Alternative Designs

Requirements analysis

As mentioned in background chapter, Upconversion Nanoparticle (UCNP) for the usage of photodynamic therapy (PDT) requires having certain functions as FDA-approved drug. As the purpose of this project, primary functions such as particle sizes and uniformity, emission brightness, and stability of ALA conjugation are fall within the scope.

Objectives

- Particle size
    - Diameter between 20 to 40nm
    - With conjugation, diameter range between 30 to 50nm
- Particle uniformity
    - Uniformity in size and shape
    - UCNP's steady action in human body
- Brighter red visible light
    - More than 1.00×10^{8} absorbance unit (A.U.)
    - Overcome reduced NIR light power after tissue penetration
- Suitable drug carrier of ALA
    - Delivery of ALA conjugation
    - Stable ALA conjugation

Alternative designs

In order to properly evaluate the effects of different design components, it was critical for the team to perform research on each and every step of the production process. As a result, the team was able to identify three main core components that were essential for the core of UCNPs. (*Wilhelm, Hirsch, Schueucher, Mayr & Wolfbeis, 2012*) They are Thulium (Tm), Erbium (Er), and Hydroxide (OH^-). As a first step, the team produced a synthesis of β – 99.5%Yb 0.5%Tm for the core of the nanoparticle. Since Tm Nanoparticles have significant blue emission, which is an ideal design to use as ultraviolet (UV) test.

99.5% Yb, 0.5% Tm (alpha phase)

In a 50ml flask, 0.1365g of Sodium Trifluoro-acetate (NaTFA), 1.3 mg of Thulium Trifluoro-acetate (TmTFA), and 0.2547g of Ytterbium Trifluoro-acetate (YbTFA) are added and mixed with 1.43g of Oleic Acid (OA), 2.53g of Octadecene-1 (ODE), and 1.34g of Oleyamine (OAm). By using temperature controller and magnetic stirrer, the flask was heat up to 110℃ for degasing. With this degasing process, it would promote release of any extra and unnecessary gas between molecules and helps its purity and reaction time. During this process, bubbles occurred in the fluid and disappeared after couple of minutes. After 10 minutes of degasing process, the temperature was controlled to 300℃ to initiate alpha phase of the nanoparticle. This process lasted for 35minutes to fully transform the fluid into alpha phase nanoparticles. Ytterbium Trifluoro-acetate (Yb^{3+}TFA) functions as main core, TmTFA as activators, and NaTFA as size controller. After the heating process, the team let the fluid to be fully cool down as low as 70℃. Then it was centrifuged and all the fluid residue were removed. With the centrifuged alpha phase nanoparticles were diluted with 10ml of Hexane. Alpha phase nanoparticles can be checked with its particles sizes and uniformity by having either Transmission Electron Microscopy (TEM) images, which will be explained further below, taken or simple 980nm Laser test. For the 980nm Laser test, increasing laser power more than 2 Ampere will show light emission to estimate its uniformity and sizes.

Transmission Electron Microscopy

Transmission Electron Microscopy (TEM) uses a beam of electrons to transmit through a thin nanoparticle specimen. Using the interaction of the electrons, it filters into black and white images to show detailed images. Since the average sizes of UCNPs were approximately between 15nm to 100nm, TEM was the only microscopy that allowed accurate confirmation of particle size. Nanoparticle sample fluids were then placed in circular shaped carbon mesh with a diameter of 2mm. The carbon mesh was then inserted into the vacuum of the TEM, manipulating controllers to determine the best locations to take images. For UCNPs, 160,000× zoom was recommended to get an image for the particle comparison.

99.5% Yb, 0.5% Tm (beta phase)

Once the alpha phase of the nanoparticle production was complete, the team moved onto the beta phase. Once all the hexane was dried, 0.1365g of NaTFA was added to the flask. Then, a solvent of 2.83g of OA and 2.53g of ODE were added. An ultrasonic bath diluted both the NaTFA and the dried alpha phase particles. The degassing process utilized in the alpha stage was repeated for 10minutes. Afterwards, the temperature of the solution was set to 325℃ for 30minutes in order to properly transform the Beta cores. To obtain the pure beta phase nanoparticles, the centrifugation and dilution with hexane steps from alpha stage were repeated. TEM imagery was then repeated to verify uniformity and size as well as the 980nm laser test with 0.5amperes. The 10ml of beta phase core nanoparticles were then diluted in hexane. The team transferred half of the nanoparticles (5ml) into a 50ml flask. Once the solution was fully dried of all hexane, the pure core nanoparticles were then mixed with 10% Yb, and 90%Y with 0.068g of NaTFA. 2.83g of OA and 2.53g of ODE were also added to function as solvents. The flask was then heated first to 110℃ for 10min for degasing and then heated to 325℃ for 30min, similar to the heating process in the beta phase production of the cores. Both Centrifugation and dilution of hexane were performed identically to the beta phase core production. After the transfer of the UCNPs into hexane into a 20ml glass vial, TEM imagery and 800nm wavelength laser tests were conducted as shown in figure 7 below.

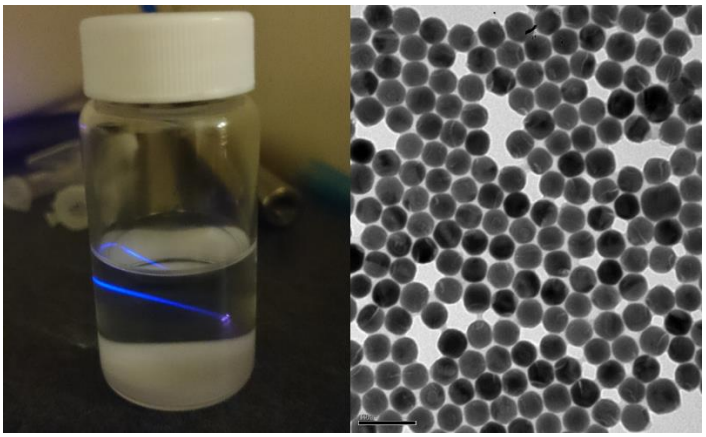

Figure 7. 99.5%Yb 0.5%Tm Core nanoparticle with laser and TEM imaging

These procedures including both alpha and beta phases are considered as the basic preparation for producing UCNPs. Having a shell around the beta phase nanoparticle causes higher energy transfer and creates brighter emission with different wavelength laser.

For example, core nanoparticle already has an emission occurs at 980nm wavelength laser. However, Addition of Nd in shell ingredient will make the nanoparticles to be emitted at 800nm wavelength laser with the same color of emission as the core had originally.

99.5% Yb, 0.5% Tm (Shell production)

99.5% Yb and 0.5% Tm with Neodymium (Nd) Shell resulted in significant blue emission, which cannot be used for the team's purpose of this project. Because red emission from UCNP will be required to activate photosensitizers, the team had to come up with alternative designs of UCNP with biocompatibility and increased red emission.

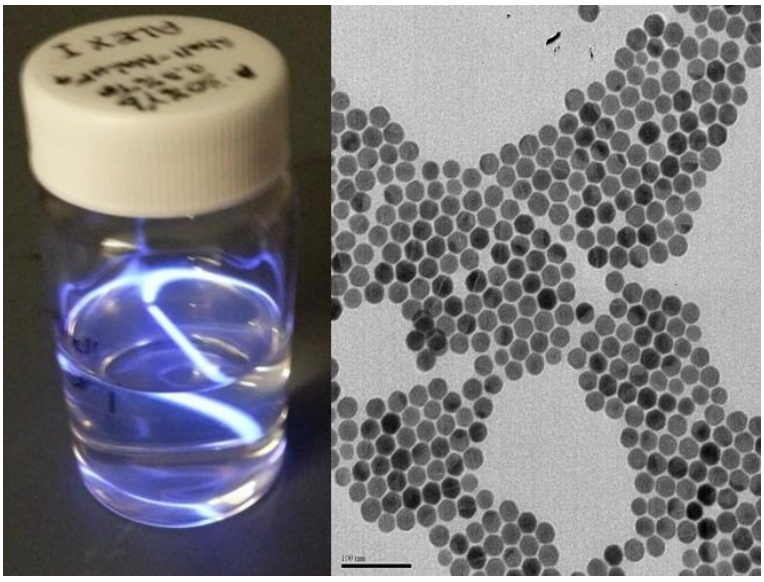

Figure 8. 99.5%Yb 0.5%Tm Core with $NaYF_4$ shell nanoparticle with laser and TEM imaging

CaF_2 Shell nanoparticles (80%Yb 2%Er core)

Over the course of research, the team began to consider CaF_2 nanoparticles which consist of the same compounds as human bone tissue. The nanoparticles also emit red light which served as an ideal model to work with the team's planned experiments such as penetration tests and imaging. A CaF_2 nanoparticle study showed 80%Yb and 2%Er core had the best red emission with fluorescent testing. The team began production of 80%Yb and 2%Er CaF_2 nanoparticles.

To produce the CaF_2 nanoparticles, the team had to follow a continuous production method from alpha phase into shell without the beta phase. 50 ml three neck flasks with 2.26g of OA and 2.02g of ODE, and 15ml two neck flasks with 5.1mg of Er, 0.068g of NaTFA, 0.2050g of YbTA, and 0.385g of YTFA with their solvents of 1.42g of OA and

1.27g of ODE were put in the heating plates at 110℃ for the degas process. Prior to the 10 minutes of degasing process, the team performed ultrasonic bathing for the 15 ml flask with solutes in order to fully dilute. After the degas, 50 ml three neck flasks were heated up to 310℃, in order to activate the forming alpha phase process. The success of the process was confirmed by the change of color from clear to yellow. Then with 5ml syringe, the team transferred all of the degased fluid from the 15ml flask to 50ml flask with its temperature of 310℃ to start the alpha phase. During the transfer process, the fluid was slowly and continuously injected into the 50ml flask over the duration of 5minutes. After completing the transfer, the combination of two fluids was kept at a temperature of 310℃ for an hour. While they were forming alpha phase nanoparticles, the team prepared a mixture of 0.5320g of Calcium Trifluoro-acetate (CaTFA) as solutes and 1.42g of OA and 1.27g of ODE as solvents for the CaF_2 shell production. The fluid went through the degasing process at 110℃ twice with Argon injection in-between the two processes.

After one hour of alpha phase nanoparticle production, half of the CaF_2 shell fluid, approximately 1.5ml, was transferred into 50 ml three neck flask with its same method the team took as previous fluid transfer with a syringe. Transferring 1.5ml of the fluid at a continuous speed for 3minutes activated shell production around the alpha phase nanoparticles. After 30minutes of shell production at a consistent temperature of 310℃, the second half of the fluid from 15ml flask was transferred into 50ml three neck flask in order to promote the stability of the shell. The purpose of separating shell fluid injection into two different steps was to increase the chemical bonding structure of shell to be more stable and evenly spread around all the alpha phase nanoparticles. 30minutes after the second injection, the team removed the heating plate and fully cooled down the fluid to as low as 70℃. After the cooling process was complete, the fluid was transferred into a 50 ml conical centrifuge tube and centrifuged at 7,000rev/min for 10minutes and all fluid residues was removed. The centrifuged alpha phase nanoparticles were then diluted with 10ml of Hexane. TEM imagery and a 980nm laser test were conducted to determine particle uniformity and size. The team confirmed the red emission of the UCNPs, which aligned well with the planned experiments. In order to confirm with the CaF_2 study of 80%Yb 2%Er, the team produced each different ratio of particles as shown in figure 9.

Figure 9. Alternative designs; CaF_2 nanoparticles comparison with different ratio of Yb; 20%, 40%, 60%, 80%, and 98% respectively

As a result, TEM Images showed different molecule structure as Tm activated cores. As previously showed in figure 7 and 8, Tm Cores and shells had a uniformed circular shape of particles. However, CaF_2 shell particles had very distinctive square shapes in figure 10 below. Each particle sizes fell under the given size range of 20 to 40nm as stated in objectives. 20%, 40%, 60%, 80%, and 98% Yb composed alternative designs had average diameter size of 26, 25, 26, 26, and 28nm respectively.

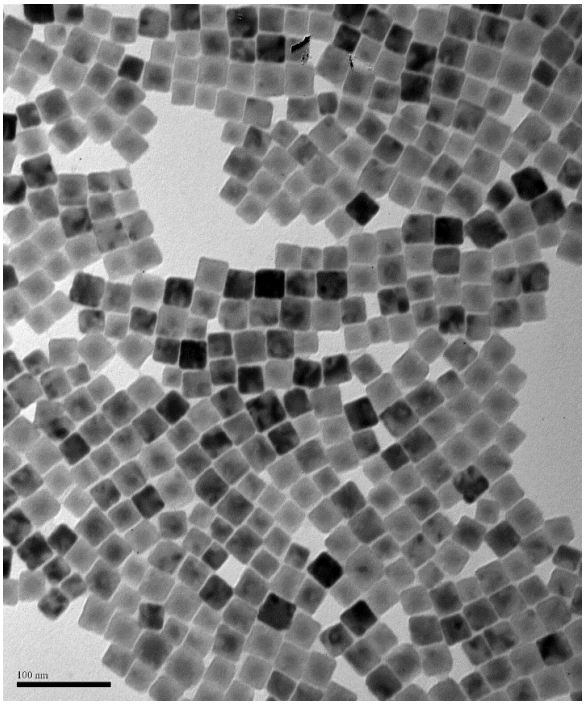

Figure 10. TEM image of CaF2 nanoparticle with 80%Yb 2%Er

After confirming nanoparticles' size and uniformity with TEM images, the team proceeded to move on the experimental processes with CaF_2 nanoparticle with 80%Yb 2%Er.

ALA Coupling

With the advantage of nanotechnology, the team combined ALA-PDT by developing upconversion nanoparticles (UCNPs), which were excited by near infrared light (NIR) and emitting multicolor to ultraviolet. In this case, the red right needed to activate PpIX carried by the UCNP providing better deep tissue penetration.

In chapter 4 mentioned how the team developed α-$NaYF_4$:Yb,Er with a biocompatible CaF_2 shell for imaging applications. Being a component of ossified tissues, CaF_2 is even more compatible than the conventional NaYF4 shell on UCNPs. The team had amplified the red emission of NaYF4:Yb,Er@CaF_2 by adjusting the ratio of the core Yb^{3+}.

Emission spectra under CW 980nm 1 W/cm3 excitation was obtained and corresponding photographs of these UCNPs demonstrated chapter 4, it was discovered α-NaYF4:80%Yb,2%Er@CaF_2 had the optimal red emission with 980nm light excitation required for the PpIX to produce singlet oxygen and induce tumor death, as seen in-vitro with simulated deep-tissue conditions.

The team conjugated 5-ALA to the UCNPs by using covalent hydrazine linkage to avoid pre-leakage of the ALA that would increase the success of the therapy by increasing its bioavailability in figure19 demonstrate the process of conjugating ALA-on αNaYF4:80%Yb,2%Er@CaF_2.

Using a 4ml vial, 1ml of α-NaYF4:80%Yb,2%Er@CaF_2, 4ml hexane, 5ml dimethylformaide (DMF) and 2g of Nitrosonium tetrafluoroborate ($NOBF_4$) were added and mixed for 24h using a magnetic stirrer. After 24 hours took the vial contents are poured into conical tube, then the vial was washed with a total of 10ml isopropanol ensuring no particles are left behind. Using the counter top centrifuge the conical vial was balanced and centrifuged for 10min at 7000rpm. After 10min supernatant decanted and small pellet formed. The vial contained the pellet-dissolved in10ml of the DMF using sonicator, and then added to 30ml single neck flask and 10mg/ml (100mg) of polyacrylic acid (PAA). The

flask was placed in an oil tube resting on a temperature/ stirrer controller, temperature set on 80^{o}C using a 1000rpm for another 24 hours.

The contents, after 24 hours, are poured into conical tube, washed the single neck flask with a total of 30ml hexane and 30ml isopropanol and transferred into the same vial. The vial was then centrifuged-using 11,000rpm for 30min at temperature of 20^{o}C. The pellet formed was dissolved in 10ml deionized water and centrifuged-using 11,000rpm for 30 minutes and 20^{o}C, this step was repeated twice by the third centrifuge, the pellet re-solubilized in 5ml phosphate buffer saline (PBS) and centrifuged using the same settings previously, this step was repeated twice eliminating the pellet from any free PAA.

The solution was then transferred into glass vial, where 0.05g 1-Ethyl-3-(3-dimethylaminopropyl)-carbodiimide (EDC) and 0.025g N-hydroxysulfosuccinimide (Sulfo-NHS) is added to the glass vial and left on the stirrer for two hours. The contents were transferred into the conical tube and centrifuged using the centrifuge settings above. After completing the centrifuge time, the pellet dissolved in 5ml PBS using the sonicator later transferred into glass vial and placed under the hood on a stirrer, carefully 5ml of hydrazine transferred into the glass vial and closed immediately which left to react for 24 hours.

The final step before conjugating the ALA, using the contents from the previous reaction and centrifuged using 11,000rpm, for 30minutes under 20℃ temperature, the pellet was then solubilized and centrifuged twice in 5ml deionized water using sonicator to make absolutely sure there was no free hydrazine on the UCNPs. After the last wash 5ml of methanol and acetic acid was added, repeated twice by following the earlier centrifuge settings using the usual settings to make sure there was no water and only methanol and acetic acid in the solution. The contents were transferred into glass vial covered with aluminum with stir bar, added 4ml of ALA and placed on a medium-high speed stirrer for 48 hours.

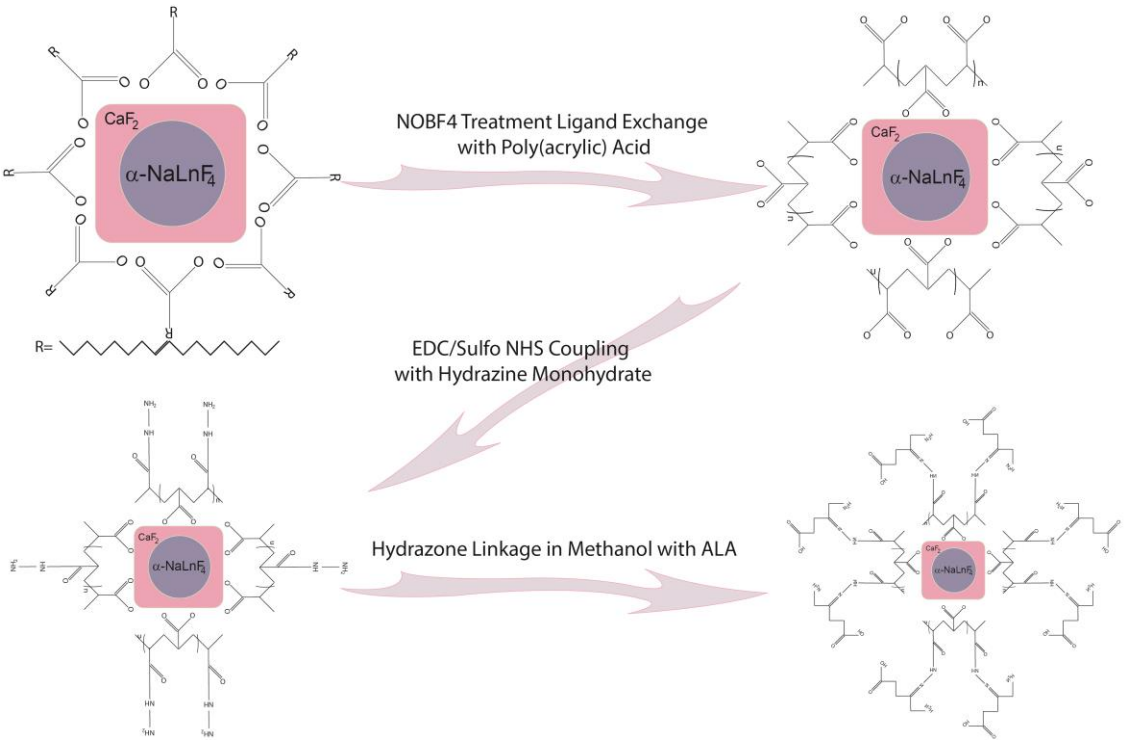

Figure 11. The Process of Conjugating 5-Aminolevulinic acid on αNaYF4:Yb80%Yb,2%Er@CaF2

There are two reasons why the ALA-UCNPs are attracted to cancers cells. One, the ALA is an amino acid, carbon based and naturally occurring; therefore the body will not recognize it as a furan body and reject it. Second, the hydrazine is composed of two amino groups and has a positive charge nitrogen. Since the UCNPs-ALA have a charge of -7mv, which is less negative than the cells -40mv ALA-UCNPs they are phagocytized by the cell and exposed to the low pH of the endosome. This caused the cleavage of the hydrazine linkage and the ALA subsequently diffused to the mitochondria causing the overproduction of PpIX. Meanwhile, the leftover Hyd-UCNP in the endosome would remain unharmed and be activated by the NIR light, leading to the photosensitization of PpIX and death for the cell shown in figure 12.

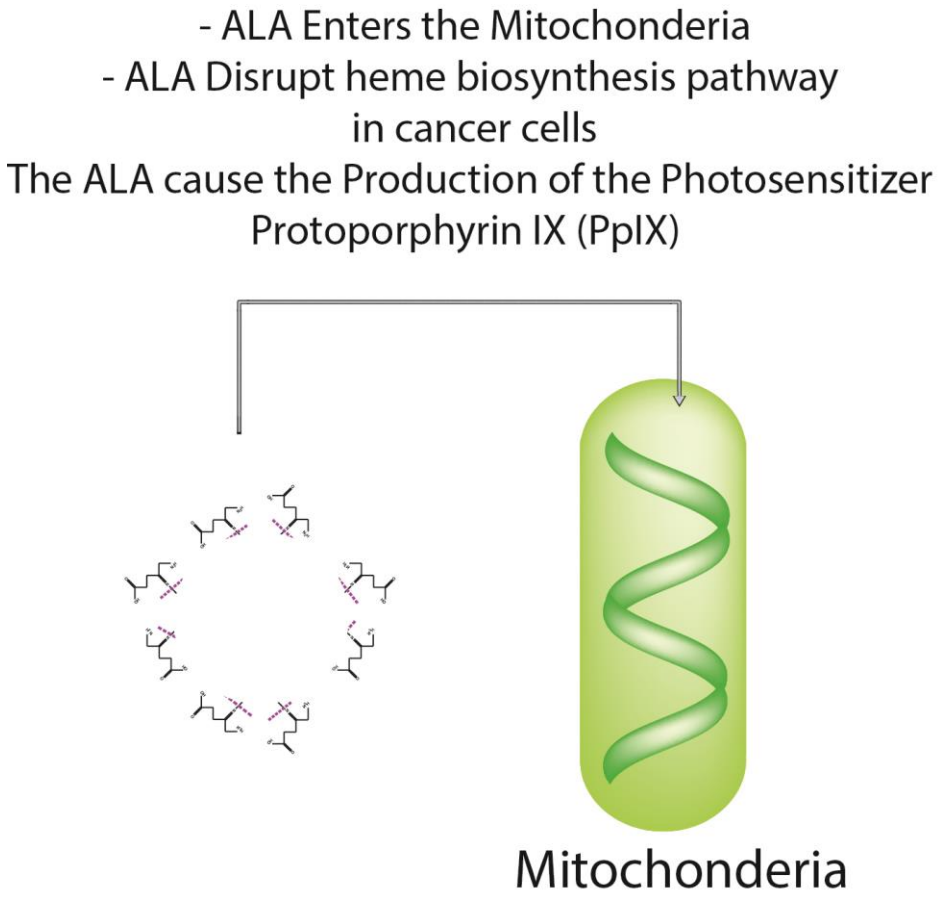

Figure 12. Illustration demonstrating the Production of PpIX in the mitochondria

Using the final chosen nanoparticle α-NaYF4:Yb(80%),Er(2%)@CaF_2 conjugated with 5-Aminolevulinic acid (ALA), several experiments were performed to determine the consistency of the size using the TEM. A fluorometer was utilized to measure the red emission of the ALA-UCNPs in both water and hexane, and Fourier Transform Infrared Spectroscopy (FTIR) was used to confirm the conjugation of the ALA to the UCNPs via a hydrazine linkage. Then Methylthiazol Tetrazolium Assay (MTT) was performed to measure the cell viability and cell imaging demonstrating the generation of reactive oxygen species (ROS)

Chapter 5: Design Verification

Transmission Electron Microscopy (TEM):

Emission spectra under CW 980nm 1W/cm^2 excitation and corresponding photographs of these Upconversion Nanoparticles (UCNP) demonstrated that as the Ytterbium (Yb^{3+}) core-doping ratio increased from 20% to 80% and that the red emission increased dramatically in figure 13a-b. Integrated counts between 600 and 700nm indicated a 250% percent increase in red emissions from α-NaYF4:20%Yb,2%Er@CaF2 to α-NaYF4:80%Yb,2%Er@CaF2 shown in figure 13c below. Furthermore, the red emissions of α-NaYF4:80%Yb,2%Er@CaF2 was 15 times stronger than that of ß-NaYF4: 20%Yb,2%Er@NaYF4.

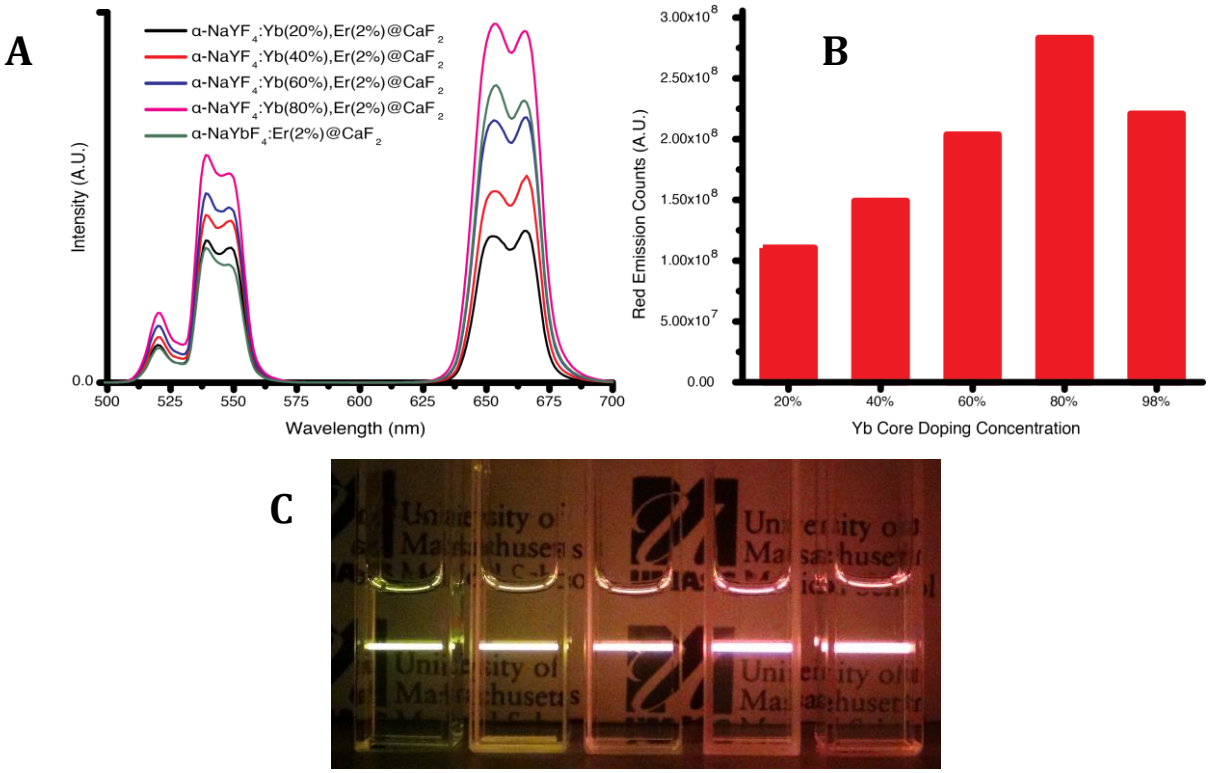

Figure 13. Emission spectra (a) under CW 980 nm 1 W/cm2 excitation and photographs (b) of α-NaYF4:Yb,Er@CaF2 UCNPs with different Yb-levels (c) Integrated counts of red emission of α-NaYF4:Yb,Er@CaF2 UCNPs with different Yb-levels.

TEM images in figure 14a,b,c below showed that the conjugation process formed mono-disperse UCNPs in water and the dynamic light scattering determined the hydrodynamic size of UCNP with 5-Aminolevulinic Acid (ALA-UCNP) conjugation was about 62.66nm which was appropriate for tumor accumulation.

Additionally, PAA-UCNPs in water exhibited less than 25% quenching in red emission from UCNPs in hexane, which indicated that the UCNPs would efficiently play the role of NIR-to-Red visible light transducer for the endogenous protoporphyrin IX (PpIX) shown in figure 14d,e below.

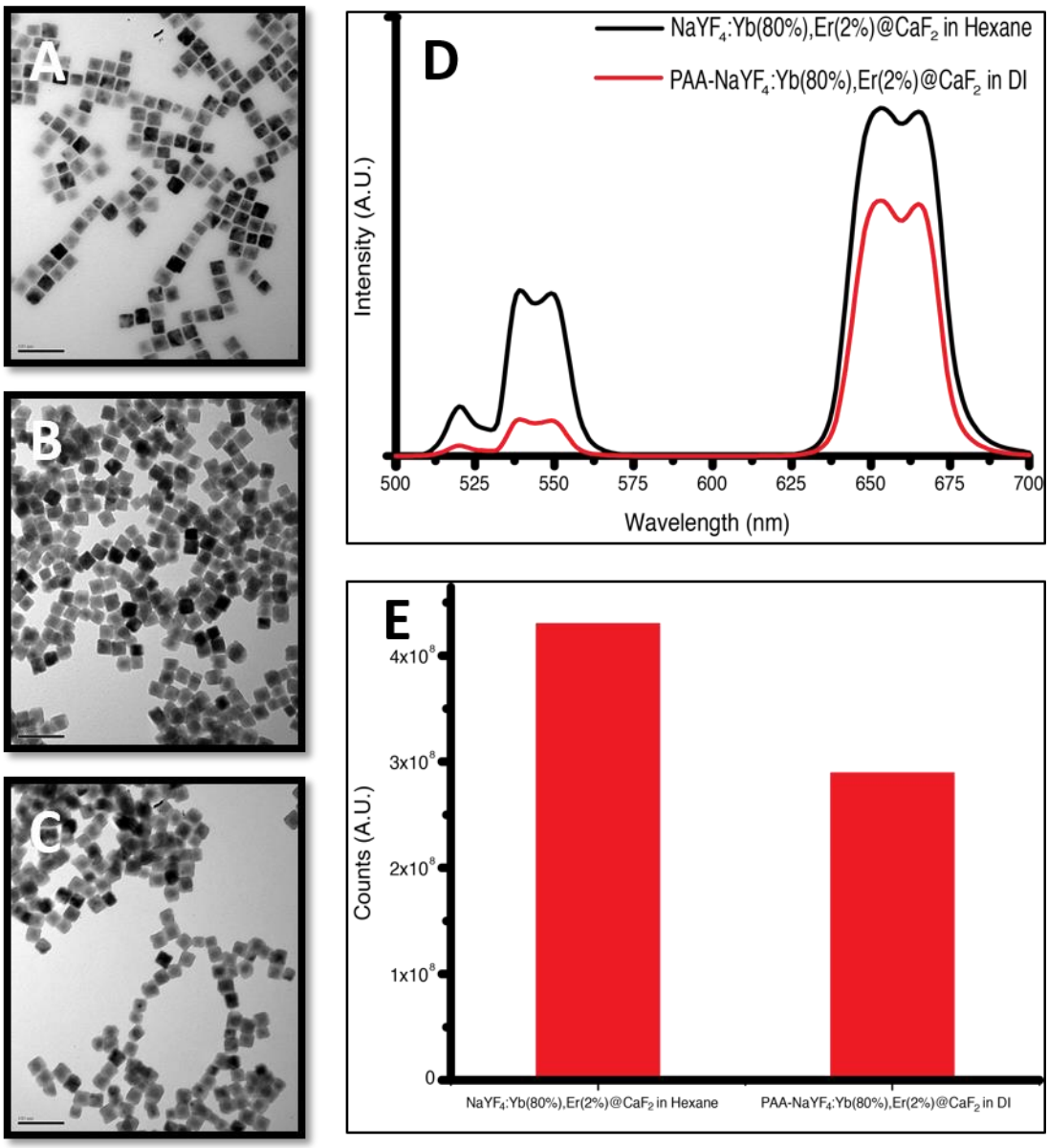

Figure 14. Characterization of hydrophilic UCNPs: TEM images of PAA-UCNPs (a), Hyd-UCNPs (b), ALA-UCNPs (c). Emission spectra of hydrophilic PAA-UCNPs in distilled water and hydrophobic OA-UCNPs in hexane, both at 10mg/mL (e) and integrated counts of their red emission indicating about 30% quenching.

Fourier Transform Infrared Spectroscopy (FTIR) Spectral Analysis

FTIR spectral analysis was employed to confirm the conjugation of ALA to the UCNPs via a hydrazine linkage. Using an agate mortar and pestle, a 3mg of each sample

PAA-UCNPs, Hyd-PAA-UCNPs and ALA-Hyd-PAA-UCNPs were obtained and individually grinded with 100mg potassium bromide (KBr) until they formed a fine powder. Each sample was then transferred to the center of the filter paper, where a circle shape was cut-off and leveled equally filling the entire circle. O-rings were placed on the top where the pellet was pressed. Pressure was released after 3 minutes and then the disk was carefully removed from the mold as shown in figure 15a,b,c.

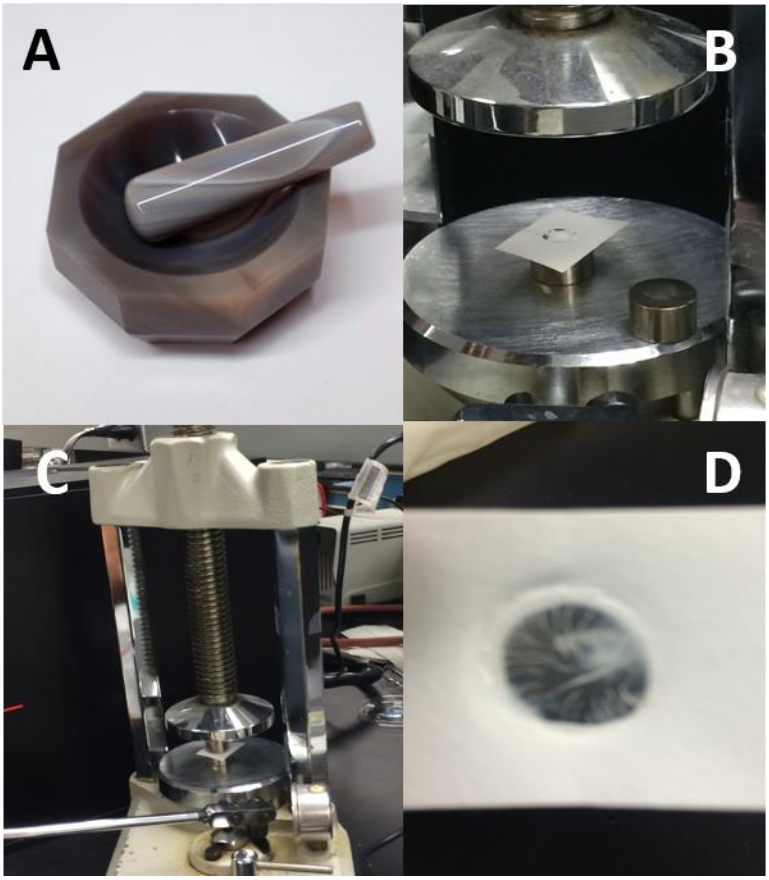

Figure 15. Images of the FTIR Process

On the spectrum for PAA-UCNPs, the peak at 1636cm^{-1} was attributed to the resonance of the carboxyl groups. However, this peak disappeared after its amidation with hydrazine, as two new peaks at 1550 and 1408cm^{-1} arose. These were attributed to the N—H bending and stretching vibrations of NH3+ respectively. Finally, when the hydrazine linkage to ALA was constructed, the peak at 1628cm^{-1} represents the —N=C— bond between the hydrazine-functionalized UCNPs and the ALA and the retention of the peak at 1550 cm^{-1} indicated the full acid-sensitive covalent linkage was successfully constructed between the ALA and the UCNPs in figure 16.

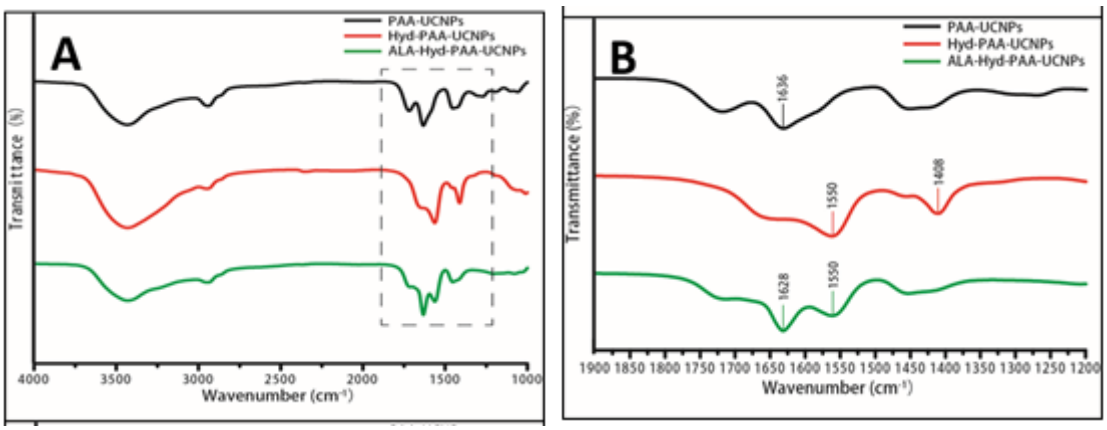

Figure 16. Full FTIR spectra (A) and partial detailed spectra (B) of PAA-, Hyd-, and ALA-UCNPs.

High-Performance Liquid Chromatography (HPLC) Analysis:

To determine the loading efficiency After the ALA-conjugation process and centrifugation of fresh ALA-UCNPs, the methanol-based supernatant was saved and vacuum dried and leftover solutes (including un-conjugated ALA) were re-dispersed in 2mL deionized (DI) water. This solution was evaluated with HPLC to determine the concentration of free ALA by a standard curve (264 nm detection wavelength)

Table 1. Concentration Calculation

	1 M pure ALA	80%
Retention Time	1.89 m	1.93 m
264 nm	5174.89	1453.84
210 nm	10875.09	2846.25

Average concentration calculated based on two-wavelength detection:

80% sample ALA concentration: 0.28 M.

Methylthiazol Tetrazolium (MTT) Assay:

To validate the therapeutic potential of the ALA-conjugated UCNPs, an MTT cell proliferation assay was implemented in which HeLa cells were exposed to ALA-UCNPs and various controls (all 100µg/mL) for 4 hours followed by irradiation of continuous wave (CW) 980 nm light at 1 W/cm2.

A 96-well microtiter plate seeded with 1x104 HeLa cells/well was incubated overnight at 37℃ with 5% Carbon dioxide (CO_2). Cells were subsequently exposed to 100µg/mL of ALA-UCNPs, Hyd-UCNPs, ALA, or PBS for 4 hours and then irradiated

with CW 980nm laser diode at 1W/cm2 for 0, 5, 10, or 20 minutes. After overnight incubation, cells were labeled with 12mM solution of MTT in PBS for 4 hours. Finally, the media was aspirated and replaced with 50µL DMSO and a plate reader at 540nm determined the formazan absorption.

Cell viability data as shown in figure 17 have a time-dependent curve for cells exposed to ALA-UCNPs, resulting in almost 70% cell killing after 10minutes, while controls had minimal cytotoxicity.

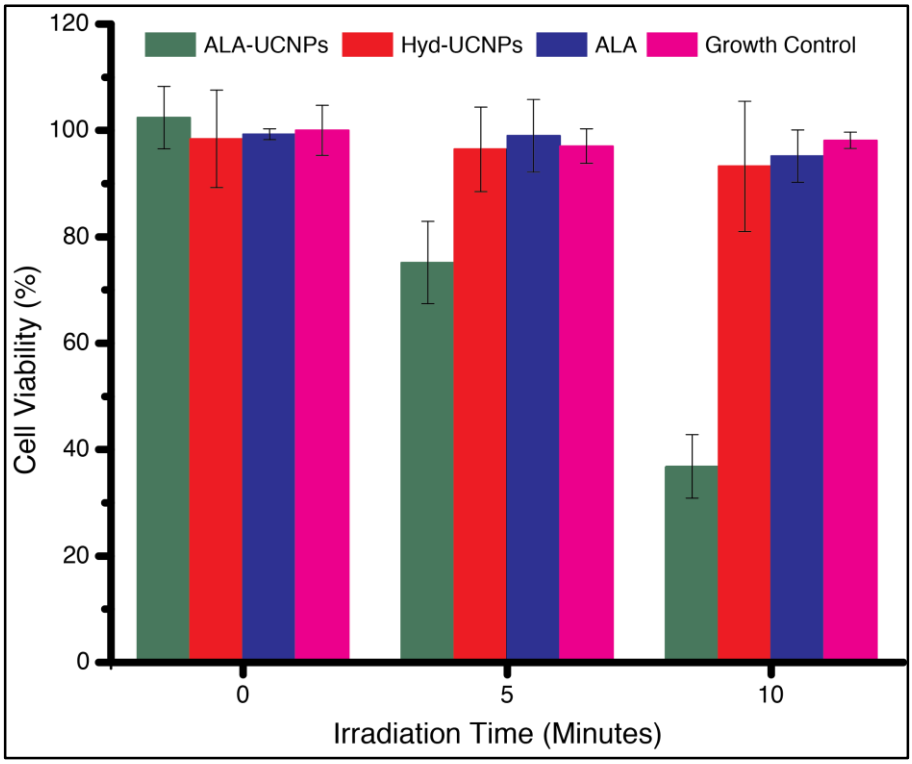

Figure 17. HeLa cell viability exposed to ALA-UCNPs (100 µg/mL), Hyd-UCNPs (100 µg/mL), free ALA (100 µg/mL), and nothing (growth control) and irradiated with CW 980 nm light at 1W/cm2 power density.

Cell Viability Exposed to 20% and 80% (MTT Assay)

Furthermore, the red-emissions of α- NaYF4:Yb(80%),Er(2%)@CaF2 was 15 times as strong as that of ß-NaYF4:Yb(20%),Er(2%)@ ß-NaYF4, as shown in figure 13 the supposed optimal red-emitting UCNP structure. As shown in figure 18, the team preformed MTT assay to see the effect of changing in Yb^{3+} concentration on cell viability as shown in figure 18 below.

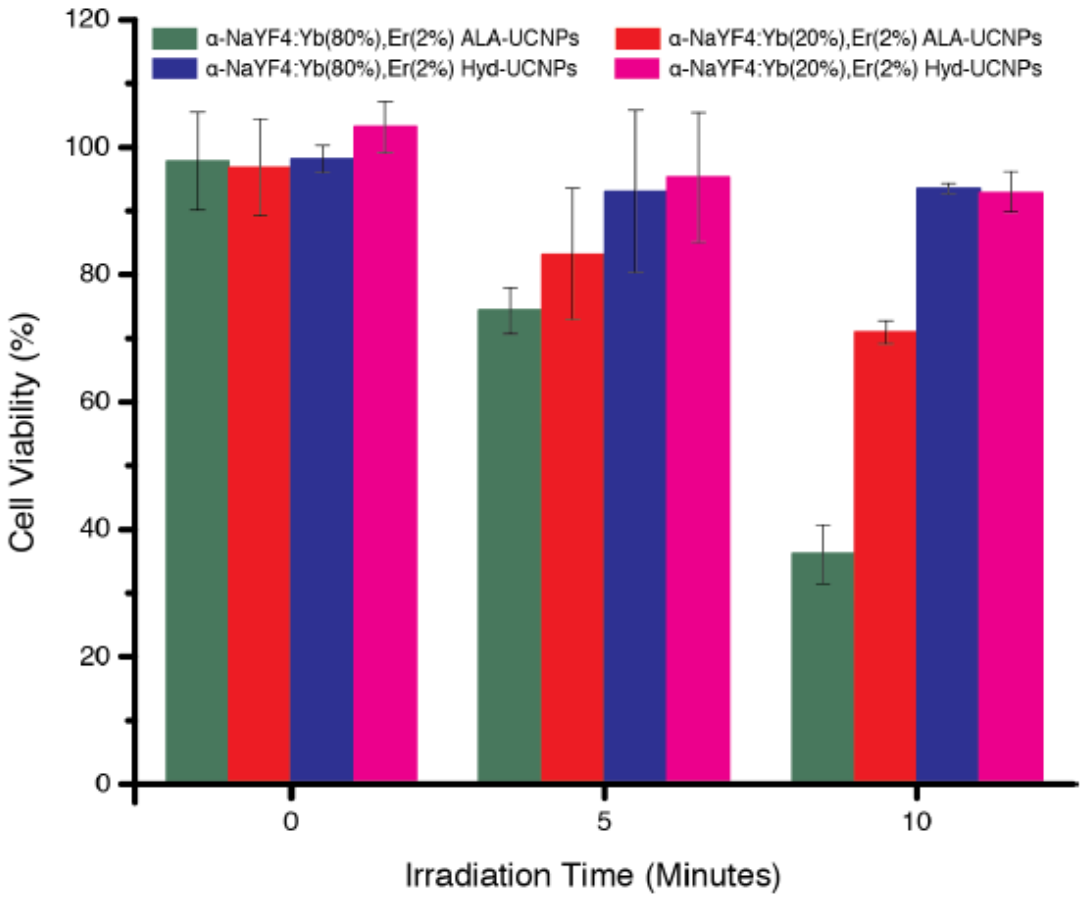

Figure 18. HeLa cell viability exposed to 20% Yb and 80% Yb ALA-UCNPs (100 µg/mL) and 20% Yb and 80% Yb Hyd-UCNPs (100 µg/mL) and irradiated with CW 980 nm light at 1W/cm2 power density.

Singlet Oxygen Detection Cell Imaging

The team validated the production of PpIX and concomitant generation of singlet oxygen species caused by exposure to ALA-UCNPs. The team stained cells with 2', 7' –dichlorofluorescein diacetate (DCFDA), a standard fluorescent indicator for singlet oxygen generation, and imaged using fluorescence microscopy as shown in figure 19. DCFDA diffuses into the cell and is acetylated into a non-fluorescent compound by cellular esterase. Reactive oxygen species (ROS) oxidizes it into 2', 7' –dichlorofluorescin (DCF), which has bright green fluorescence.

Singlet Oxygen Detection Cell Imaging: Glass-bottom confocal dishes seeded with 1×10^6 HeLa cells were incubated overnight at 37℃ with 5% CO_2. Cells were subsequently exposed to 100µg/mL of ALA-UCNPs or Hyd-UCNPs for 4 hours. Cells were washed three times with warmed Hank's Balanced Salt Solution (HBSS) and then stained with

25μM DCFDA in HBSS for 45 minutes. Using a fluorescent microscope equipped with a CW 980nm laser diode at 1W/cm^2, DCFDA fluorescence was imaged with 495nm excitation and 535nm emission between 0, 5, and 10minutes of irradiation using a 60× water-immersion objective lens.

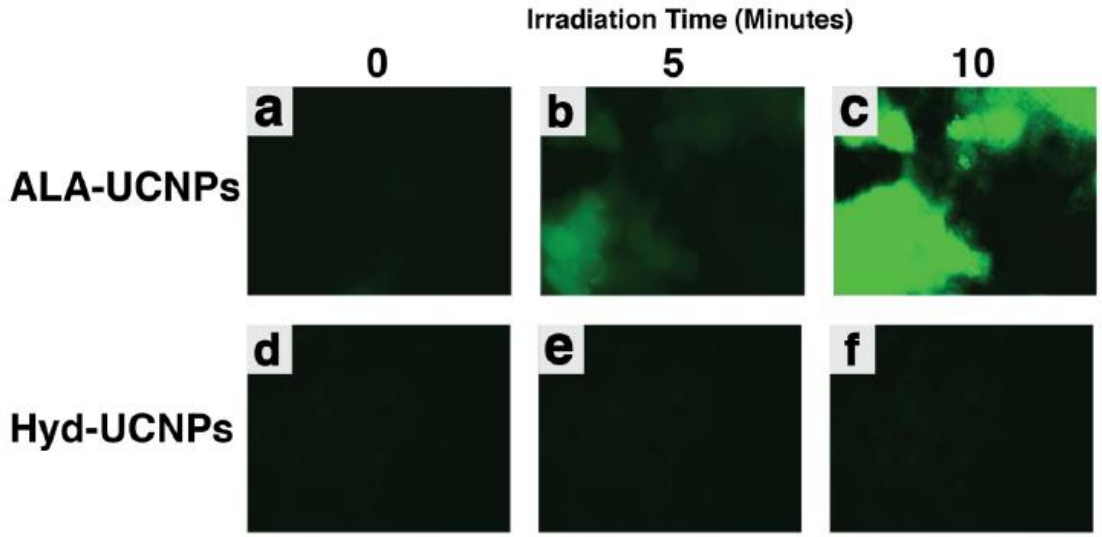

Figure 19. Singlet oxygen production detected by fluorescence of DCFDA in HeLa cells exposed to 100 μg/mL of ALA-UCNPs and irradiated with 0 (a), 5 (b), and 10 (c) minutes of CW 980 nm light at 1W/cm2 power density. Singlet oxygen production detected by fluorescence of DCFDA in HeLa cells exposed to 100 μg/mL of Hyd-UCNPs and irradiated with 0 (d), 5 (e), and 10 (f) minutes of CW 980 nm light at a 1W/cm2 power density.

Singlet Oxygen Detection Quantification

Singlet Oxygen Detection Quantification: A 96-well micro-titer plate seeded with 1×10^4 HeLa cells/well was incubated overnight at 37℃ with 5% CO_2. Cells were subsequently exposed to 100μg/mL of ALA-UCNPs, Hyd-UCNPs, ALA, or PBS for 4 hours and then stained with 25μM DCFDA in HBSS for 45minutes. After irradiation with CW 980nm laser diode at 1W/cm^2 for 0, 5, or 10 minutes, DCFDA fluorescence was immediately determined with a plate reader with 495nm excitation and 535nm emissions.

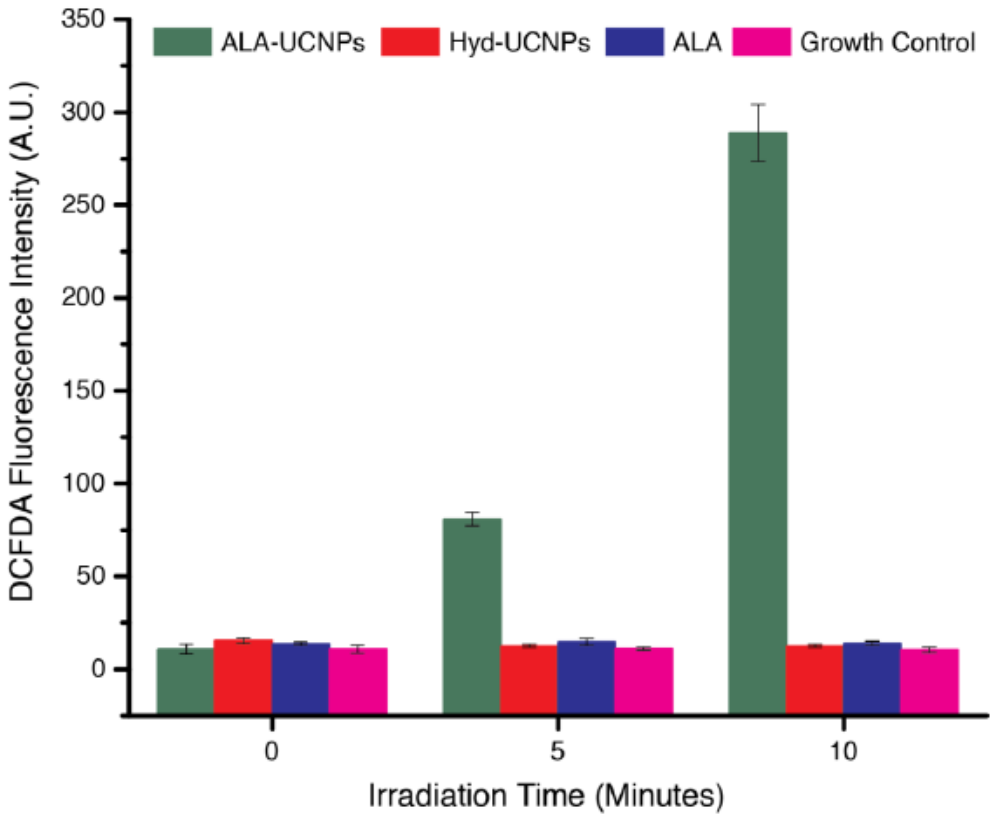

Figure 20. Singlet oxygen quantified by DCFDA fluorescence in HeLa cells exposed to 100µg/mL of ALA UCNPs, Hyd-UCNPs, ALA, and nothing (growth control).

MTT Assay with Porcine Tissue

Once the team achieved effective results using the 80% Yb, PDT was used to stimulate in deep tissue. In this regard, pieces of tissue of varying thickness were placed between the NIR laser and HeLa cells exposed to UCNPs figure 21a, and analyzed for cell viability with an MTT assay figure 21b. Exposure time was 20 minutes of 980nm irradiation at $1W/cm^2$ under same condition mentioned in previous MTT test. It is also worth noting that with the added distance between the meat and cells, the height of the well and the media bathing the cells, the simulated depths were greater than the measured thickness of the tissue.

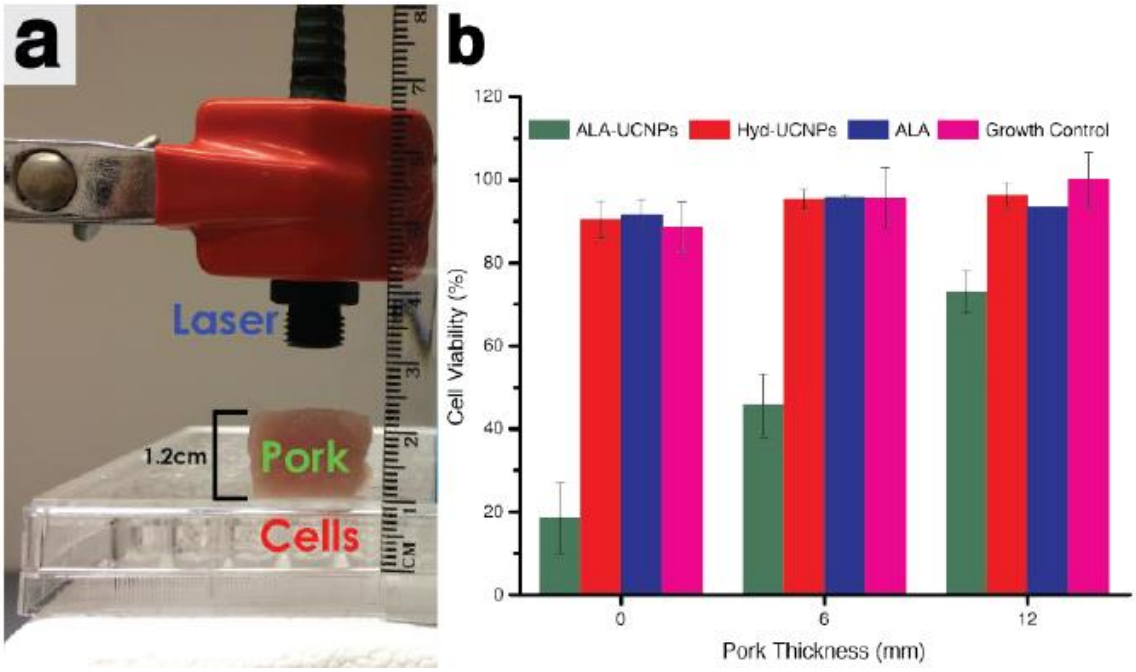

Figure 21. Photograph of the setup of simulated visceral tumor conditions in an in vitro MTT assay (a). HeLa cell viability exposed to ALA-UCNPs (100 µg/mL) and Hyd-UCNPs (100µg/mL) and irradiated with CW 980nm light at a 1W/cm² power density for 20 minutes

Chapter 6: Discussion

Photodynamic Therapy (PDT) with Upconversion Nanoparticles (UCNP) has been used in many studies as a potential cancer treatment and showed promising results. As such, it has been considered as an alternative treatment for current cancer treatments like chemotherapy, radiotherapy and surgery. However, current techniques are limited by the efficiency of the treatment with respect to tissue penetration. This project has demonstrated a new technique being studied to increase tissue penetration by increasing red light emission through the use of PDT with $NaYF_4$:80%Yb,2%Er@CaF_2 UCNPs, which are responsible for the activation of the 5-Aminolevulinic Acid (ALA) drug photosensitizer (PS). Ytterbium (Yb^{3+}) plays an essential role in changing the amount of red light emission. Previous studies showed that 20% Yb^{3+} produces the best red emission, while the team found that 80% Yb^{3+} gives off the highest red light emission compared to different percentages of Yb^{3+}, as figure 21 illustrates. The team confirmed these results through a variety of tests that showed the low toxicity of UCNPs, the best red emission intensity by using NaYF4:80%Yb,2%Er@CaF_2, and the successful and effective ALA conjugation which prove that ALA-conjugated UCNPs have therapeutic potential.

Viability and Effectiveness of UCNPs-ALA for PDT as cancer treatment

In order to use $NaYF_4$:80%Yb,2%Er@CaF_2 UCNPs as an effective activator and drug carrier for ALA, the team tested the size of UCNPs, red light emission, the amount of ALA conjugation with UCNPs and tested the cell viability. Figure 14 shows results from Transmission Electron Microscopy (TEM) imaging that portray the average size of UCNPs 37nm (Standard Deviation of 3nm) which is in the desired range for physiological testing (*Xueyuan, 2014)*. To determine the best red emission intensity that UCNPs are able to produce, different percentages of Yb were used to make UCNPs. Figure 13a,b show emission spectra under continuous wave (CW) 980nm 1W/cm^2 excitation and Yb^{3+} core-doping ratio increases 20%, 40, 60, 80, and 98% respectively. 80% Yb^{3+} produced the highest red light emission compared to other percentages**.** Figure 13c is a photograph of the UNCPs emitting. Figure 13 illustrates **i**ntegrated counts between 600 and 700nm indicating that there is a 250% percent increase in red emissions from α-$NaYF_4$:Yb20%Yb,2%Er@CaF_2 to α-$NaYF_4$:Yb80%Yb,2%Er@CaF_2, which means that

the red light emissions of α- $NaYF_4$:Yb80%Yb,2%Er@CaF_2 are 15 times stronger than that of ß $NaYF_4$:Yb20%Yb,2%Er@$NaYF_4$. The importance of red emission is that the PTD photosensitizing drug is activated under red emission and in the actual experimental process, the team was using the ALA as a photosensitizing drug.

After the team found that α-$NaYF_4$:Yb80%Yb,2%Er@CaF_2 had the optimal red emissions, ALA-conjugated α-$NaYF_4$:Yb80%Yb,2%Er@CaF_2 were synthesized via the process represented in figure 11. In cellular experimentation, the ALA-UCNPs were expected to be phagocytized by the cell and exposed to the low pH of the endosome. This would cause the cleavage of the hydrazine linkage causing the ALA to diffuse to the mitochondria and cause an overproduction of Protoporphyrin IX (PpIX) as shown in figure 12. During this process the leftover Hyd-UCNP in the endosome would remain unharmed within the cells and be activated by the NIR light, leading to the photosensitization of PpIX, which will produce singlet oxygen ($1O_2$) and cause the death of the tumor cell. Therefore, high red light emission is an important factor in PDT with UCNPs treatment, because red light is the excitation light that activates UCNPs which will trigger ALA and activate PpIX. The stronger this light is, the deeper its effective distance will be, so it can be used for deep cancer treatment.

After ALA conjugation with UCNPs the team performed various tests to check if ALA successfully conjugated to the UCNPs and to verify the amount of ALA that was conjugated. First the team tested if the ALA were successfully conjugated to UCNPs by a Fourier transform infrared spectroscopy (FTIR) test and the results demonstrated the existence of ALA on UCNP surfaces as shown in figure 16. When the hydrazine linkage to ALA was constructed, the peak at 1628cm^{-1} represents the —N=C— bond between the hydrazine-functionalized UCNPs and the ALA and the retention of the peak at 1550cm^{-1} indicates that the full acid-sensitive covalent linkage was successfully constructed between the ALA and the UCNPs. The second test was High-Performance Liquid Chromatography (HPLC), which was used to test the concentration of ALA after ALA conjugation with HYD-UCNPs. The results in figure 17 showed that UCNPs 80%Yb-ALA with an ALA concentration of 0.28M, exhibited a loading capacity of the ALA is 48.26μmol/10mg in the HYD-UCNPs, approximately 50% of the initial amount.

After testing the conjugation of ALA with HYD-UCNPs by FTIR and calculating the concentration of ALA by HPLC, the team determined that there is a sufficient amount of ALA to be used as an effective cancer drug in in-vitro tests, and further, in-vivo testing.

The team performed Methylthiazol Tetrazolium (MTT) Assay which is used to demonstrate multiple facts, firstly to test the toxicity of UCNPs because they will be used for human testing and secondly to determine the effectiveness of ALA as a drug to kill cancer cells as the team used Hela cells. Figure 17 shows Cell viability data which shows that exposing cells to ALA-UCNPs resulted in almost 70% cell death after 10 minutes, while UCNPs-HYD showed close similarity to control results, demonstrating that UCNPs have low toxicity by themselves and proving that ALA works successfully with UCNPs as a cancer treatment. UCNPs were exposed to cells for four hours before the tests were performed under CW 980nm 1W/cm^2 excitation.

The team tested the effect of using different Yb^{3+} concentration on the emission of red light as figure 13 demonstrated using 80%Yb^{3+} increase red light emission 15 time more than 20%Yb^{3+}. The team performed MTT assay to see the affect in changing Yb^{3+} concentration on cell viability, as figure 18 shows 80%Yb^{3+}ALA-UCNPs had 70% decrease in cell viability while 20%Yb^{3+}ALA-UCNPs had 30% decrease in cell viability, the team's results clearly show that increases in Yb^{3+} concentration has critical effect on cell viability.

Throughout research, the team found that cells exposed to ALA-UCNPs show intensifying DCFDA fluorescence over irradiation time, clearly indicating the production of PpIX and then singlet oxygen shown in figure 19 a-c. This data was later corroborated with a quantification of the singlet oxygen production by measuring the fluorescence intensity of the Cellular Reactive Oxygen Species Detection (DCFDA) using 96-well micro-titer plate reader in figure 20. Both DCFDA fluorescence imaging and micro-titer plate measurement suggest effective prodrug delivery and subsequent PpIX activation by the red emitting UCNPs.

Finally, once the team had established the optimal red-emission and PDT effect of 80% Yb^{3+} UCNPs, simulating PDT in deep-set tumor conditions was desired. After 20 minutes of irradiation at 1W/cm2, all tissue thicknesses had cell viabilities significant to the control (Hyd-UCNPs). While no tissue (0mm) resulted in less than 20% cell viability,

6mm had less than 50% cell viability and 12mm had less than 80% cell viability. This establishes and validates the feasibility of using UCNPs as a NIR-to-Red visible light transducer for prodrug photodynamic therapy at a deep-tissue level (thickness greater than 1cm).

Even after ALA conjugation, UCNP size was around 62nm which is still in the acceptable range to be used in human testing and appropriate for tumor accumulation, as TEM images show in figures 14a,b,c**,** the conjugation process formed a uniform size and distribution of ALA-UCNPs in water. Since ALA will form an extra layer on the UCNPs the team tested emission spectra of UCNPs before and after ALA conjugation and the results showed that PAA-UCNPs in water exhibit less than 25% quenching in red emission from UCNPs in hexane, indicating the UCNPs are the main factor in NIR-to-Red visible light transducer for the endogenous PpIX as shown in figure 14d,e.

UCNPs for PDT as a cancer Treatment: A larger perspective

Economics

It is well known that cancer treatment is one of the most expensive treatments used in the medical field. Among the 12 drugs approved by the Food and Drug Administration for various cancer conditions in 2012, 11 were priced above $100,000 for a year of treatment, and since 2010 the median price has been around $10,000 (*Levy*, *2013*). Despite their extreme cost, current cancer drugs do not exhibit high efficiency in the majority of cancer cases. If PDT with UCNPs were used as a cancer treatment the team believes that it will be less expensive than existing drugs, because the materials that comprise UCNPs and ALA are not expensive and there is no need for high a quantity of ALA-UCNPs due to the highly tumor targeted nature of ALA.

Societal Influence

Environmental effects are very important factor in drug manufacturing, especially with the complicated rules and laws that restrict any environmental or pollution effect. It is important to understand future effects of the disposals from both the therapy itself and also of the materials associated with its manufacturing. The production of UCNPs requires the use of lanthanide salts. Yb^{3+} and Er, current compounds used for doping, show no

environmental threat to plants or animals. They are considered biologically lifeless. Water-soluble compounds of Yttrium (Y) are considered mildly toxic, mostly affecting aquatic animals. Therefore waste disposal in the manufacturing process would need to be monitored but will not require special licensing or permits to be acquired. (*Ytterbium Oxide, 2010*) (*Erbium Oxide, 2008*).

Political Ramification

Cancer is getting everybody's attention, because cancer is the second cause of death in the US (*American Cancer Society, 2012a*). Any treatment for cancer will have big influence on the society because it will change lives and give hope to millions of people who are suffering from cancer so searching for affective and successful cancer treatment is a need for every person, because there are a lot of factors are involved in casing cancer like chemical radiation, genetic, tobacco, diet and physical activity and every single person living these days are getting exposed to one of these factor which mean everyone is under the risk of having cancer.

Health and Safety

Safety was a major objective of the design and has been addressed with toxicity analyses in-vitro. As for any treatment, the health and safety of the patient is of the highest importance. The ultimate goal of PDT with UCNP-ALA would be to kill cancer cells without affecting other tissues. The drug is designed to specifically target tumor cells without negatively affecting the health of any other organ system, and with minimal side effects.

Ethical Concern

The main goal of this project is to find alternative cancer treatment for current treatment by using PDT with UCNPs-ALA. This would directly improve the lives of all patients receiving the treatment and minimal the side effects that occur due to current cancer treatments. The ethical concerns that are usually raised are related to marketing, administration, and availability of the treatment. During the marketing process it should be carefully done so that the expectations of patients do not exceed the limitations of the treatment. Patients need to be informed about potency and limitations of the drug, and what the treatment does and how it works. Administration of the treatment has to be noninvasive

so patient does not have to suffer during treatment. To ensure the level of pain and the risks, animal models should be used. Since cancer is a global problem, the treatment needs to be made available on multiple continents and would have to be accessible for all demographics. Therefore, efforts must be made to keep production costs affordable in the international markets.

Chapter 7: Final Design and Validation

As mentioned above, cancer is fatal disease that does not yet have a viable cure. There is a pressing need to find an effective preventative treatment. Heretofore, the team proposed a design that utilizes Upconversion Nanoparticle conjugated with 5-aminolevulinic acid (ALA-UCNP) with Photodynamic Therapy (PDT) to treat cancer by killing cancer cells in human body. However, producing cancer treatment faces a lot of challenges in regards to safety, scalability, efficacy, and specificity.

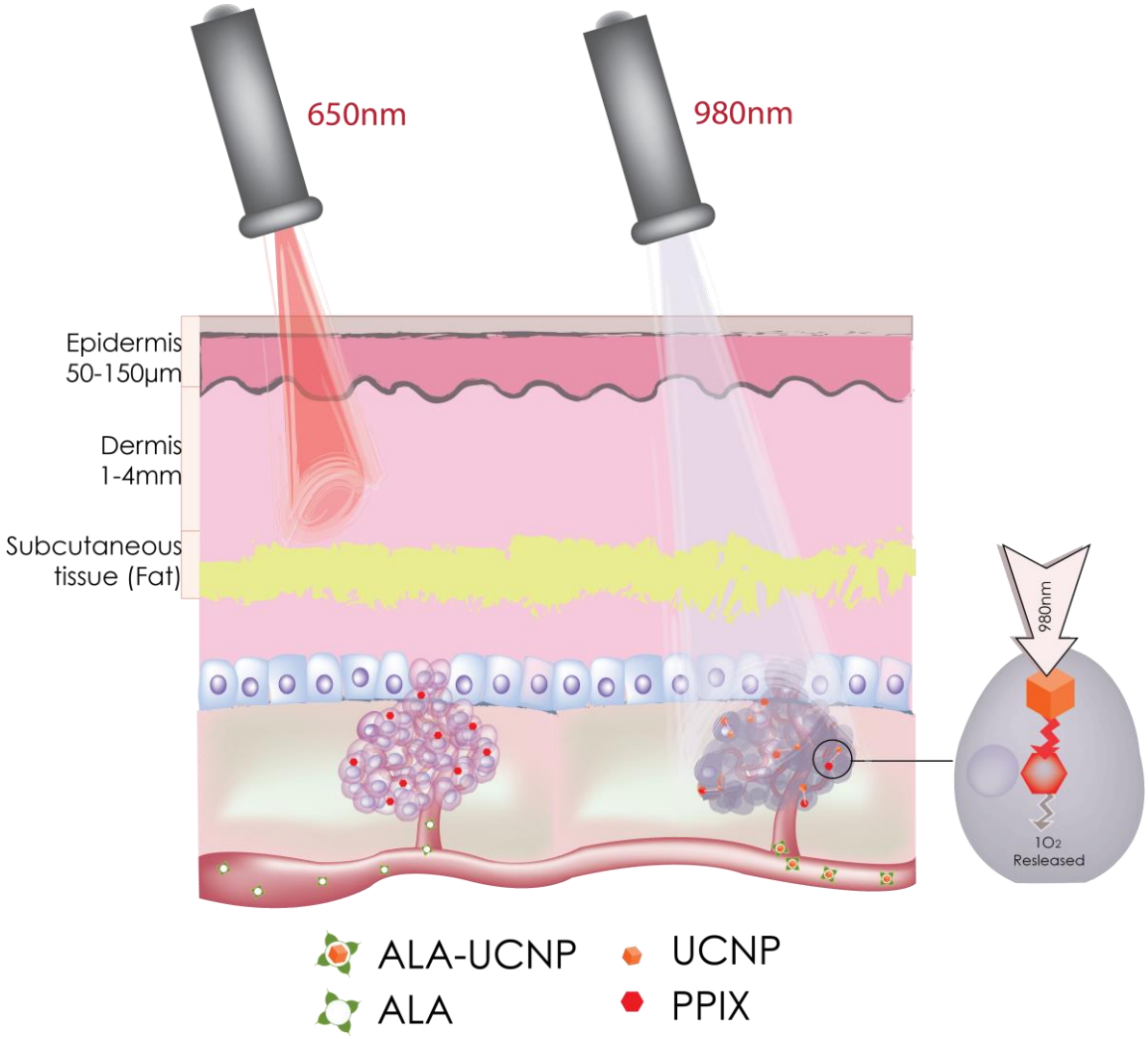

Figure 22. Schematic of the final design components and its work mechanisms.

The goal of this project was to find alternative treatment for cancer by enhancing current PDT and making it more effective for cancer therapy, especially for deep cancer. The main problem with the current PDT procedure is the penetration depth and, as figure 22 shows, that the current PDT use 650nm wavelength to activate ALA and produce singlet

oxygen. In order to enhance the light penetration and reach deeper tissue, the team used UCNPs as transducer which will convert 980nm NIR to red visible light and activate ALA to produce singlet oxygen as shown in figure 22. The team successfully synthesized ALA-UCNPs and found the best red light emission by using 80%Ytterbium (Yb^{3+}). Over the course of this project, the team was able to demonstrate hypothetical PDT system with various experiments, which showed effective and significant results which strongly make PDT with UCNPs as real alternative cancer treatment with great potentials.

Thus, the specific objectives of this study were to assess the application of novel UCNPs as ultraviolet (UV) light emitter to activate ALA is to increase tissue penetration by increasing red light emission which was demonstrate by increasing the percentage ratio of Yb^{3+} in UCNPs.

In order, their priority was determined to evaluate the success of the design:

1. Specificity
2. Scalability
3. Safety
4. Efficacy

To make sure that the team's progress is directed by scientific criteria and as the results of simple experiments would guide the parameters chosen for more complex procedures. Below, experiments are described in the chronological order in which they were performed, with the reasoning for experiment prioritization:

1. Safety was evaluated first because low cytotoxicity was a constraint for this project; the cytotoxic effects of the UCNPs should not compromise cell viability below 90%. Therefore, Methylthiazol Tetrazolium (MTT) assay tested the cytotoxicity and it was first experiment conducted to ensure that future experiments fell within acceptable particle dosages. Following cytotoxicity assays, team test the size of UCNPs to make sure they fall in the range of 50nm to 60nm to be used in physiological testing.
2. Testing the red light emission that produces from UCNPs was next measure test that the team conducted in this project, because the main goal of this project is to increase the red emission to solve the limitation that current UCNPs have. In effect, data from these tests enabled the team to scale the amount of Yb^{3+} that used in producing UCNPs

and at the end chose the best percentage Yb^{3+} ratio which will help the team maintaining maximum design efficiency.

3. The FTIR and HPLC experiments were performed next, to gauge the efficacy of the design by testing if ALA conjugated to UCNPs. Therefore these tests show that UCNPs are capable to be used as drug carrier, which would indicate the specificity of the delivery system in or design.
4. To demonstrate the efficacy of the team's design, MTT assay was utilized if ALA working effectively as cancer drug by increment cell death during 980nm wavelength laser exposure.

The cell line chosen to conduct these studies was the HeLa human cervical cancer line. All cultures were maintained and prepared using antibiotic-free, DMEM+10% FBS. All assays were performed in standard tissue culture polystyrene and incubated at 37^{o}C 21% Oxygen (O_2) and 5% Carbon Dioxide (CO_2). All cell counts were determined by hemocytometer, without using trypan blue exclusion staining.

Chapter 8: Conclusions and Recommendations:

Conclusions

The experimental approach showed the possibilities of several features of Calcium Fluoride (CaF_2) shell Upconversion Nanoparticle's (UCNP) in vitro activity. After considering alternative designs for biocompatibility, one of the biomaterials; CaF_2 was chosen as the design component. Regarding UCNP's design selection, Transmission Electron Microscopic (TEM) images were used to measure particle size and uniformity for each design samples with different percent of Ytterbium (Yb^{3+}) component. Particle sizes of 30 to 50nm diameter are allowed for biological usage and met the design objectives. All of the samples passed particle size and uniformity requirements in the initials process of the experiment series.

CaF_2-shell UCNPs with 20%, 40%, 60%, 80%, and 98% component of Yb^{3+} were measured their emission spectra through fluorometer. As a result, CaF_2-shell with 80% Yb^{3+} had the strongest red emission, which was approximately about 3.00×10^8 A.U. Using the selected alternative design, 5-Aminolevulinic Acid (ALA) and hydrazine conjugation was performed for better water solubility and release of singlet oxygen ($1O_2$) to kill target cells. Two different conjugated samples were checked for usability through TEM and fluorometer tests. The results showed hydrophilic PAA-UCNP were still emitting enough brightness, at nearly 3.00×10^8 A.U. With a uniform particle size of about 40nm.

In addition, Fourier Transform Infrared Spectroscopy (FTIR) confirmed the conjugating condition of ALA and Hydrazine. Then Methylthiazol Tetrazolium (MTT) Assay was preformed to demonstrate that UCNPs having low cytotoxicity, 98% cell viability after 10minutes of exposure to 980nm wavelength laser with Hydrazine UCNPs. On the other hand, ALA UCNP showed about 30% cell viability on the same MTT assay, which proves theory of CaF_2 UCNP with ALA Functionality are right. Along with MTT Assay, fluorescence intensity images of cells proved about 7 times bigger size of the cells were produced of singlet oxygen in the cells. After verified the major photodynamic therapy with ALA conjugated UCNP, MTT assay of alternative designs showed CaF_2-shell UCNP with 80% Yb^{3+} had the most cell died during 10minutes of 980nm wavelength laser exposure. As the last experiment, MTT assay with tissue penetration test resulted less than

60% cell viability in 6mm thickness of tissue and less than 80% cell viability with 12mm thickness tissue after 10 minutes of exposure of 980nm wavelength laser.

This proves that this engineered biocompatible CaF_2-shell showed 15-fold increment in red emission compared with current one. Also, ALA-conjugation, which was a prodrug for red-absorbing photosensitizer protoporphyrin IX (PpIX) to the UCNP, allows great control of its release in the cell. In-vitro test of this photodynamic therapy system was performed to prove its therapeutic potential such as cell viability of ALA conjugated UCNPs and release of toxicity via photosensitizer.

Recommendations

Under the limitation of time scope such as UCNP production, conjugation, and experimental process time, this study was limited into partial requirements to become an outstanding product for actual pharmaceutical usage. The implementation of following recommendations might expand and develop the current characterization of ALA-UCNP for cancer treatment.

1. **Repeat experiments in more alternative UCNPs.** Due to the delicate process of UCNP production, each UCNP sample had slight differences on its size and emission. In order to get more accurate and detail data, more sample of UCNP need to be tested.
2. **Conduct experiments with in vivo tests.** After concluding the project, experiments showed promising results of ALA conjugation with CaF_2-Shell UCNP in PDT. In vivo testing will show great chance of proving its potential in its pharmaceutical usage.
3. **Repeat experiments with different laser power.** During the course of experimental process, 980nm wavelength laser approximately $1W/cm^2$ power was used. Over-heating effects regarding using this laser power with UCNP was rarely observed.
4. **Repeat experiments with Zinc-PCA conjugation.** Both ALA and Zinc-PCA have great function of photosensitizing. Due to the limited research and experiment time, the experimental processes were limited into ALA conjugation.
5. **Possible over-heating concerns.** Throughout these experiments, the team did not discover any significant problem of over-heating effect during the experiments. As

the length of the Laser wave gets longer, it causes more over-heating effect due to the hydrogen in human tissue. Since the team proved that 980nm wavelength was strong enough to penetrate 12mm of tissue, further study needs to be proceeded in order to find out the smaller wavelength laser such as 800nm or 750nm wavelength.

References

- *American Cancer Society, "Cancer Facts & Figures 2013." 4 Sept. 2012a. Web. 26 Sept. 2013. <http://www.cancer.org/research/cancerfactsfigures/cancerfactsfigures/cancer-facts-figures-201>.*
- *American Cancer Society, "Learning About New Cancer Treatments." 4 Sept. 2012b. Web. 26 Sept. 2013. <http://www.cancer.org/treatment/treatmentsandsideeffects/complementaryandalternativemedicine/learningaboutnewcancertreatments/learning-about-new-ways-to-treat-cancer-toc>.*
- *Auzel, F. (2004). Upconversion and anti-Stokes processes with f and d ions in solids. Chemical reviews, 104(1), 139-174.*
- *Castano, A. P., Mroz, P., & Hamblin, M. R. (2006). Photodynamic therapy and anti-tumour immunity. Nature Reviews Cancer, 6(7), 535-545.*
- *Chen, G., Shen, J., Ohulchanskyy, T. Y., Patel, N. J., Kutikov, A., Li, Z., ... & Han, G. (2012). (α-NaYbF4: Tm3+)/CaF2 Core/Shell Nanoparticles with Efficient Near-Infrared to Near-Infrared Upconversion for High-Contrast Deep Tissue Bioimaging. ACS nano, 6(9), 8280-8287.*
- *Chen, Xueyuan, Yongsheng Liu, and Datao Tu. "Lanthanide-Doped Luminescent Nanomaterials." (2014).*
- *Carling, C. J., Nourmohammadian, F., Boyer, J. C., & Branda, N. R. (2010). Remote-Control Photorelease of Caged Compounds Using Near-Infrared Light and Upconverting Nanoparticles. Angewandte Chemie International Edition,49(22), 3782-3785.*
- *Dougherty, T. J., Gomer, C. J., Henderson, B. W., Jori, G., Kessel, D., Korbelik, M., ... & Peng, Q. (1998). Photodynamic therapy. Journal of the National Cancer Institute, 90(12), 889-905.*
- *Erbium Oxide; MSDS No. 25883 [Online]; Acros Organics N.V.: Fair Lawn, NJ,November 20, 2008, http://fscimage.fishersci.com/msds/25883.htm (accessed December 2, 2011).*
- *Fingar, V. H. (1996). Vascular effects of photodynamic therapy. Journal of clinical laser medicine & surgery, 14(5), 323-328.*
- *Haase, M., & Schäfer, H. (2011). Upconverting nanoparticles. Angewandte Chemie International Edition, 50(26), 5808-5829.*
- *Idris, N. M., Gnanasammandhan, M. K., Zhang, J., Ho, P. C., Mahendran, R., & Zhang, Y. (2012). In vivo photodynamic therapy using upconversion nanoparticles as remote-controlled nanotransducers. Nature Medicine.*

- *Jayakumar, Muthu Kumara Gnanasammandhan, Niagara Muhammad Idris, and Yong Zhang. "Remote activation of biomolecules in deep tissues using near-infrared-to-UV upconversion nanotransducers." Proceedings of the National Academy of Sciences 109.22 (2012): 8483-8488.*
- *Kalka, K., Merk, H., & Mukhtar, H. (2000). Photodynamic therapy in dermatology. Journal of the American Academy of Dermatology, 42(3), 389-413.*
- *Liu, Y., Tu, D., Zhu, H., Ma, E., & Chen, X. (2013). Lanthanide-doped luminescent nano-bioprobes: from fundamentals to biodetection. Nanoscale, 5(4), 1369-1384.*
- *Levy, Alison Rose. "The Sky-High Price of Chemotherapy: Why Do Cancer Drugs Cost So Much?" TakePart. N.p., 09 May 2013.*
- *Mader, H. S., Kele, P., Saleh, S. M., & Wolfbeis, O. S. (2010). Upconverting luminescent nanoparticles for use in bioconjugation and bioimaging. Current opinion in chemical biology, 14(5), 582-596.*
- *MOAN, J., & Peng, Q. (2003). An outline of the hundred-year history of PDT. Anticancer research, 23(5A), 3591-3600.*
- *Oleinick, N. L., Morris, R. L., & Belichenko, I. (2002). The role of apoptosis in response to photodynamic therapy: what, where, why, and how. Photochemical & Photobiological Sciences, 1(1), 1-21.*
- *Sharman, W. M., Allen, C. M., & van Lier, J. E. (1999). Photodynamic therapeutics: basic principles and clinical applications. Drug discovery today, 4(11), 507-517.*
- *Shen, J., Chen, G., Vu, A. M., Fan, W., Bilsel, O. S., Chang, C. C., & Han, G. (2013). Engineering the Upconversion Nanoparticle Excitation Wavelength: Cascade Sensitization of Tri-doped Upconversion Colloidal Nanoparticles at 800 nm. Advanced Optical Materials.*
- *Wang, C., Cheng, L., & Liu, Z. (2013). Upconversion nanoparticles for photodynamic therapy and other cancer therapeutics. Theranostics, 3(5), 317.*
- *Wang, F., Banerjee, D., Liu, Y., Chen, X., & Liu, X. (2010). Upconversion nanoparticles in biological labeling, imaging, and therapy. Analyst, 135(8), 1839-1854.*
- *Wang, J., Wang, F., Wang, C., Liu, Z., & Liu, X. (2011). Single-Band Upconversion Emission in Lanthanide-Doped KMnF3 Nanocrystals. Angewandte Chemie International Edition, 50(44), 10369-10372.*
- *Wilhelm, S., Hirsch, T., Schueucher, E., Mayr, T., & Wolfbeis, O. (2012). Magnetic core-shell rare earth doped nanoparticles wih tunable upconversion luminescence for sensor applications., Available from Analtyk Chemistry. (WO609-12-1)Retrieved from http://www-analytik.chemie.uniregensburg.de/wolfbeis/hirsch/Poster/Poster_Europtrode_2012_Magnetic*

_Core-Shell_UCLNPs.pdf Yang, Y., Shao, Q., Deng, R., Wang, C., Teng, X., Cheng, K., ... & Xing, B. (2012). In vitro and in vivo uncaging and bioluminescence imaging by using photocaged upconversion nanoparticles. Angewandte Chemie International Edition, 51(13), 3125 3129

- *G. Tian, W. Ren, L. Yan, S. Jian, Z. Gu, L. Zhou, S. Jin, W. Yin, S. Li, Y. Zhao, Small 2013, 9, 1929.*
- *Ytterbium Oxide; MSDS No. 96772 [Online]; Acros Organics N.V.: Fair Lawn, NJ, July 20, 2009, http://www.jtbaker.com/msds/englishhtml/d7120.htm*
- *Z. Huang, Technology in cancer research & treatment 2005, 4, 283.*
- *Q. Peng, K. Berg, J. Moan, M. Kongshaug, J. M. Nesland, Photochemistry and Photobiology 1997, 65, 235.*
- *S. Collaud, A. Juzeniene, J. Moan, N. Lange, Current Medicinal Chemistry -Anti-Cancer Agents 2004, 4, 301.*